

Ultracold collisions of molecules

Goulven Quémener

Laboratoire Aimé Cotton, CNRS,
Université Paris-Sud, ENS Paris-Saclay, Université Paris-Saclay,
91405 Orsay, France
e-mail: goulven.quemener@u-psud.fr

March 28, 2017

Abstract

This paper deals with the theory of collisions between two ultracold particles with a special focus on molecules. It describes the general features of the scattering theory of two particles with internal structure, using a time-independent quantum formalism. It starts from the Schrödinger equation and introduces the experimental observables such as the differential or integral cross sections, and rate coefficients. Using a partial-wave expansion of the scattering wavefunction, the radial motion of the collision is described through a linear system of coupled equations, which is solved numerically. Using a matching procedure of the scattering wavefunction with its asymptotic form, the observables such as cross sections and rate coefficients are obtained from the extraction of the reactance, scattering and transition matrices. The example of the collision of two dipolar molecules in the presence of an electric field is presented, showing how dipolar interactions and collisions can be controlled.

Contents

1	Introduction	3
2	The Schrödinger equation	4
2.1	The Schrödinger equation for one particle	4
2.2	The Schrödinger equation for two colliding particles	5
2.2.1	Coordinate systems	5
2.2.2	Types of collisions	8
3	In the region far from collision	10
3.1	Asymptotic form of the wavefunction	10
3.2	Observables	11
4	In the region of collision	13
4.1	Partial wave expansion	13
4.2	Coupled equations	16
4.3	Case of long-range interactions described by an electrostatic multipole-multipole expansion	19
4.4	Propagation. Log-derivative \mathbf{Z} matrix	20
4.5	Symmetry considerations	20
5	Matching the two regions	23
5.1	Reactance matrix \mathbf{K} . Relation with \mathbf{Z}	23
5.2	Scattering matrix \mathbf{S} . Relation with \mathbf{K}	24
5.3	Transition matrix \mathbf{T} . Relation with observables	26
5.4	Link to scattering of structureless particles. The central potential problem	27
6	Behaviour at ultralow energy. Scattering length and threshold laws	28
7	Application to ultracold collisions of dipolar molecules in electric fields	31
7.1	A simplified problem	31
7.2	Molecules in an electric field	34
7.3	Collisions of molecules in an electric field	36
8	Conclusion and perspectives	43

1 Introduction

The achievement of slowing, cooling and trapping atoms [1, 2, 3] to quantum degeneracy in Bose–Einstein condensates [4, 5] or degenerate Fermi gases has tremendously impacted the Atomic, Molecular, and Optical scientific community. The world of ultracold matter is governed by Quantum Mechanics. The particles move so slowly that one has enough time in an experiment to precisely control their internal structure and external motion, with for example electric or magnetic fields, electromagnetic waves and optical lattices. Ultracold atomic physics has been extensively investigated since those achievements and has led to the exploration of new quantum phenomena [6, 7, 8].

Other types of particles, such as ultracold ions, ultracold atoms in Rydberg states and ultracold molecules, are also of specific interest. In this paper we focus mainly on ultracold molecules. Compared to atoms, molecules have a much richer structure, including rotation and vibration in addition to the electronic and spin structure. In contrast to atoms which are directly cooled with lasers, it is harder to cool the molecules with the same procedure due to the lack of closed cycles of absorption and spontaneous emission, even if it can work in certain cases [9]. Other techniques are then employed [10, 11]: buffer gas cooling [12], deceleration of molecules [13, 14], Sisyphus cooling [15], association of ultracold atoms via photo-association [16, 17, 18, 19, 20], magneto-association [21, 22], and coherent transfer driven by lasers [23, 24, 25, 26, 27].

If the molecules possess permanent electric or magnetic dipole moments, they can be manipulated by electric or magnetic fields [28, 29, 30, 31]. In addition to the individual energies of the molecules the strength and orientation of the molecule-molecule interaction can also be controlled, leading to promising applications [32]. The precise control over the initial ultracold particles and their interactions can be used to engineer different quantum edifices such as dipolar particles in optical lattices. Such controlled and tunable set-ups can be used for quantum simulation to mimic the Hamiltonian of more complicated systems of condensed matter, quantum magnetism and many-body physics [33, 34, 35, 36] or to design schemes of quantum information [37, 38, 39]. Dipolar molecules can also be used for testing fundamental theories [40, 41], or to explore a novel ultracold chemistry in a fully determined way [32, 42, 43].

Once the molecules are cooled, collisions between molecules and/or atoms can then occur [28, 44, 45, 46, 29, 30]. In all cases, collisions play an important role for understanding the stability, the lifetime and the dynamics of an ultracold gas. This paper is devoted to the time-independent quantum description of collisions between two atoms or molecules with internal structure, therefore allowing for changes of the internal state during the collision. The proposed approach is general enough to describe atom-atom, atom-molecule, and molecule-molecule collisions, and we will emphasize on the latter case. As it is based on an angular expansion of the scattering wavefunction in partial waves, the formalism is specially suited for ultralow collision energies. Section 2 starts with a reminder on the Schrödinger equation for one and two particles, on the system of coordinates, and on the types of collisions. Two different parts of the colliding motion are tackled. Section 3 describes the region beyond the range of interactions where the particles hardly feel each other. The

relevant observables are introduced there. Section 4 is devoted to the zone where the particles interact. This is where the partial wave expansion of the scattering wavefunction is introduced, leading to a system of coupled equations for the radial motion. The coupled system is solved using the method of the log-derivative matrix propagation. Symmetry considerations are also invoked, linked to the isotropy of space, to the symmetrization of identical particles, or to the presence of an external field. Section 5 proceeds to the matching between the two latter regions. The reactance, scattering and transition matrices are defined and their relations with the observables are established. Section 6 describes certain properties of collisions in the ultracold regime. In Section 7, as an application, we use this formalism to study the dipolar collisions between two ultracold KRb molecules in an electric field. We show how we can simplify the full problem to restrict the physical process to its main relevant element. Two cases are explored: (i) collisions of molecules in the ground rotational state and (ii) collisions of molecules in the first excited rotational state. It is found that collision rates can be enhanced or suppressed. We conclude and give some perspectives in Section 8.

For readers that desire additional information we refer for instance to references [47, 48, 49, 50, 51, 52, 53] among many others.

2 The Schrödinger equation

2.1 The Schrödinger equation for one particle

The dynamics of a quantum particle of mass m moving in a potential characterized by the operator \hat{V} is described by the time-dependent Schrödinger equation in the $\langle \vec{r} |$ representation:

$$i\hbar \frac{\partial \Psi(\vec{r}, t)}{\partial t} = \hat{H} \Psi(\vec{r}, t) \quad (1)$$

where $\langle \vec{r} | \Psi(t) \rangle = \Psi(\vec{r}, t)$ is the wavefunction of the particle at the position \vec{r} and time t . The operator $\hat{H} = \hat{T} + \hat{V}$ is the Hamiltonian of the particle, where \hat{T} and \hat{V} are the kinetic and potential energy operators, respectively, defined as:

$$\hat{T} = \frac{\hat{p}^2}{2m} \equiv \frac{1}{2m} \left(\frac{\hbar}{i} \vec{\nabla} \right)^2 = -\frac{\hbar^2}{2m} \vec{\nabla}^2 \quad ; \quad \hat{V} \equiv V(\vec{r}, t). \quad (2)$$

Wide hats will be used to represent the quantum operators in this paper. We define the presence probability density of a particle as $\rho(\vec{r}, t) = |\Psi(\vec{r}, t)|^2$ which has unit of a volume density. This quantity determines the probability $dP(\vec{r}, t) = \rho(\vec{r}, t) d\vec{r}$ to find the particle at time t at position \vec{r} in the volume element $d\vec{r}$. The presence probability of the particle in a finite volume \mathcal{V} is $P(t) = \int_{\mathcal{V}} dP(\vec{r}, t) = \int_{\mathcal{V}} \rho(\vec{r}, t) d\vec{r}$. Since the probability of finding the particle over all space must be unity, the wavefunction has to be normalized using $\int_{-\infty}^{+\infty} |\Psi(\vec{r}, t)|^2 d\vec{r} = 1$. This normalization is possible if the wavefunction is square integrable, typically when the wavefunction represents a bound state of a particle. For a continuum state of a particle, that is when the particle is not bound in a specific space, this normalization is not possible. Several methods are used to normalize such wavefunctions for example using a

Dirac delta function in the normalization (see for example [47, 48, 49]). We define the probability current of a particle as:

$$\begin{aligned}\widehat{j}(\vec{r}, t) &= -\frac{\hbar}{2mi} \left[\Psi^*(\vec{r}, t) \vec{\nabla} \Psi(\vec{r}, t) - \Psi(\vec{r}, t) \vec{\nabla} \Psi^*(\vec{r}, t) \right] \\ &= \text{Re} \left\{ \Psi^*(\vec{r}, t) \left(\frac{\widehat{p}}{m} \Psi(\vec{r}, t) \right) \right\}.\end{aligned}\quad (3)$$

The probability density and the probability current are related by:

$$\frac{\partial \rho(\vec{r}, t)}{\partial t} + \vec{\nabla} \cdot \widehat{j} = 0. \quad (4)$$

Eq. (4) is the continuity equation showing that the probability is conserved locally, just like a charge is conserved in electrostatics. Indeed we have, from the divergence theorem,

$$\int_{\mathcal{V}} \frac{\partial \rho(\vec{r}, t)}{\partial t} d\vec{r} = \frac{\partial P(t)}{\partial t} = - \int_{\mathcal{V}} \vec{\nabla} \cdot \widehat{j} d\vec{r} = - \oint_{\mathcal{S}} \widehat{j} \cdot d\vec{S}. \quad (5)$$

The decrease (increase) in time of $P(t)$ inside the volume \mathcal{V} at time t is equal to an outgoing (incoming) flux of \widehat{j} through the surface \mathcal{S} enclosing the volume \mathcal{V} . Note that \widehat{j} has unit of a surface density per unit of time.

If the potential energy is independent of time $\widehat{V} = V(\vec{r})$, we can find a stationary solution $\Psi(\vec{r}, t)$ with a well defined energy E_{tot} :

$$\Psi(\vec{r}, t) = \psi^{E_{tot}}(\vec{r}) e^{-\frac{iE_{tot}t}{\hbar}}, \quad (6)$$

with a separation of space and time in the wavefunction. The solution is stationary since $|\Psi(\vec{r}, t)|^2 = |\psi^{E_{tot}}(\vec{r})|^2$ is independent of time. Putting Eq. (6) into Eq. (1) gives the time-independent Schrödinger equation for $\psi^{E_{tot}}(\vec{r})$:

$$\widehat{H} \psi^{E_{tot}}(\vec{r}) = \left[-\frac{\hbar^2}{2m} \vec{\nabla}^2 + V(\vec{r}) \right] \psi^{E_{tot}}(\vec{r}) = E_{tot} \psi^{E_{tot}}(\vec{r}). \quad (7)$$

It is often the case that in collisions the potential energy V is independent of time and the total energy E_{tot} is conserved. The time-independent formalism still applies when static electric or magnetic fields are present but not anymore when the fields vary in time. Similarly, the time-independent probability density and probability current are given by $\rho(\vec{r}) = |\psi^{E_{tot}}(\vec{r})|^2$ and $\widehat{j}(\vec{r}) = -\frac{\hbar}{2mi} [[\psi^{E_{tot}}(\vec{r})]^* \vec{\nabla} \psi^{E_{tot}}(\vec{r}) - \psi^{E_{tot}}(\vec{r}) \vec{\nabla} [\psi^{E_{tot}}(\vec{r})]^*]$.

2.2 The Schrödinger equation for two colliding particles

2.2.1 Coordinate systems

We consider a time-independent collision problem of a system of two composite particles $i = 1, 2$ (for example two molecules) of mass m_1, m_2 (see Fig. 1), described

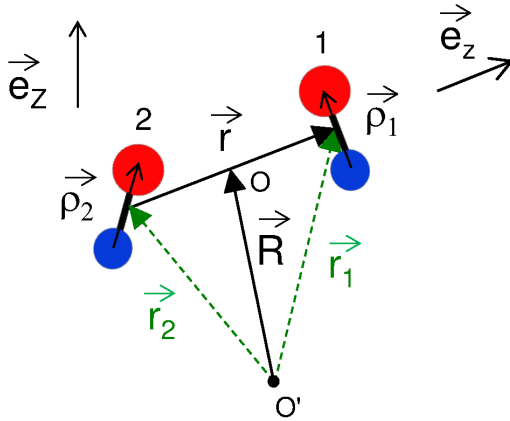


Figure 1: System of two composite particles 1 and 2 (here two diatomic molecules) described by two individual external vectors \vec{r}_1, \vec{r}_2 from an arbitrary point O' and two individual internal vectors $\vec{\rho}_1, \vec{\rho}_2$. The relative and center-of-mass vectors \vec{r}, \vec{R} are also shown. The point O defines the center-of-mass of the system. The unit vector \vec{e}_Z orients the axis OZ of the space-fixed frame while the unit vector \vec{e}_z orients the axis Oz of the body-fixed frame of the system (see text for details).

with individual external coordinates \vec{r}_1, \vec{r}_2 from an arbitrary point O' and internal coordinates $\vec{\rho}_1, \vec{\rho}_2$ (not to mistake with the presence probability density). It is also useful to introduce the center-of-mass (CM) coordinates \vec{R} and the relative (rel) coordinates \vec{r} (see Fig. 1) defined by:

$$\vec{R} = \frac{m_1 \vec{r}_1 + m_2 \vec{r}_2}{m_{tot}} \quad \vec{r} = \vec{r}_1 - \vec{r}_2, \quad (8)$$

where $m_{tot} = m_1 + m_2$ is the total mass and $m_{red} = m_1 m_2 / (m_1 + m_2)$ is the reduced mass. If we define the point O so that $\vec{O'O} = \vec{R}$, then we define a **space-fixed frame** by the axes $OXYZ$. This is the space-fixed frame of the center-of-mass of the system, we could have defined any other arbitrary space-fixed frame $O'XYZ$. Space-fixed frames are also often called laboratory frames. The axis OZ is oriented along a unit vector \vec{e}_Z as shown in Fig. 1. We did not show the other unit vectors \vec{e}_X and \vec{e}_Y that orient the axes OX and OY . We also define a **body-fixed frame** of the system by the axes $Oxyz$ when now the Oz axis is oriented along a unit vector \vec{e}_z also shown in Fig. 1, following the orientation of the vector \vec{r} . In this paper, we will choose the OZ axis as the quantization axis in the space-fixed frame and the Oz axis in the body-fixed frame of the system. The two particles interact in general via a potential energy $V(\vec{\rho}_1, \vec{\rho}_2, \vec{r}_1, \vec{r}_2)$. The particles are initially located at large distances and they start to interact as they approach from each other. They are scattered in a given direction, reflecting the strength and the anisotropy of the potential energy. In general the potential energy V of the system can be separated in two terms: a potential energy V_{int} which describes the internal interactions of the particles between themselves, and a potential energy V_{ext} which describes eventual external potentials. The former term V_{int} , contains all electrostatic Coulombic interactions

between the electrons and the nuclei of the atoms composing the system, and do not depend on the absolute position of the charges but rather on their relative separation. Using extensive ab initio calculations, the full electronic problem is solved for parametric positions of the nuclei within the so called Born–Oppenheimer approximation. It results in a potential energy term $V_{int}(\vec{\rho}_1, \vec{\rho}_2, \vec{r}_1 - \vec{r}_2) = V_{int}(\vec{\rho}_1, \vec{\rho}_2, \vec{r})$ and is usually called the **potential energy surface** of the system, as it represents an energy as a function of multi-coordinates in space. The set of vectors $(\vec{\rho}_1, \vec{\rho}_2, \vec{r})$ are often called the Jacobi coordinates. As it does not depend on the individual positions \vec{r}_1, \vec{r}_2 but only on the relative position of the molecules, it is separable in \vec{R} and \vec{r} . The latter term V_{ext} , can describe the interaction of the molecules with external fields for example a static electric or magnetic field. If these fields are uniform throughout space, these potentials do not depend on the individual positions of the molecules \vec{r}_1, \vec{r}_2 . An external potential can also depends on the individual positions of the molecules. Depending on the case, the potential can be separable in \vec{R} and \vec{r} , for example if the external potential is described by an harmonic oscillator [54], or not, for example if the potential is described by an optical lattice [55]. In the following we will consider a system described by an arbitrary potential energy surface $V_{int}(\vec{\rho}_1, \vec{\rho}_2, \vec{r})$ and an eventual external potential $V_{ext_1}(\vec{\rho}_1) + V_{ext_2}(\vec{\rho}_2)$ that does not depend on the individual position of the molecules. The total potential energy is then separable in \vec{R} and \vec{r} . The case of non-separable potentials is not treated here as it is beyond the scope of this paper. When the particles are far apart $|\vec{r}| = |\vec{r}_1 - \vec{r}_2| \rightarrow \infty$, $V_{int}(\vec{\rho}_1, \vec{\rho}_2, \vec{r}) \rightarrow V_{int_1}(\vec{\rho}_1) + V_{int_2}(\vec{\rho}_2)$, the internal potential energy of the two separated molecules 1 and 2. We define the interaction potential energy by:

$$U_{int}(\vec{\rho}_1, \vec{\rho}_2, \vec{r}) = V_{int}(\vec{\rho}_1, \vec{\rho}_2, \vec{r}) - V_{int_1}(\vec{\rho}_1) - V_{int_2}(\vec{\rho}_2), \quad (9)$$

where $U_{int} \rightarrow 0$ if $|\vec{r}| \rightarrow \infty$. Then the time-independent Schrödinger equation gives:

$$\left[-\frac{\hbar^2}{2m_1} \vec{\nabla}_1^2 - \frac{\hbar^2}{2m_2} \vec{\nabla}_2^2 + U_{int}(\vec{\rho}_1, \vec{\rho}_2, \vec{r}) + \hat{h}_1(\vec{\rho}_1) + \hat{h}_2(\vec{\rho}_2) \right] \psi(\vec{\rho}_1, \vec{\rho}_2, \vec{r}_1, \vec{r}_2) = E_{tot} \psi(\vec{\rho}_1, \vec{\rho}_2, \vec{r}_1, \vec{r}_2). \quad (10)$$

The operators $\hat{h}(\vec{\rho}_i)$ are the internal Hamiltonians of particles $i = 1, 2$:

$$\begin{aligned} \hat{h}_i(\vec{\rho}_i) \phi_{\alpha_i}(\vec{\rho}_i) &= \left\{ \hat{T}_i + \hat{V}_i(\vec{\rho}_i) \right\} \phi_{\alpha_i}(\vec{\rho}_i) \\ &= \varepsilon_{\alpha_i} \phi_{\alpha_i}(\vec{\rho}_i), \end{aligned} \quad (11)$$

where $\hat{V}_i(\vec{\rho}_i) = V_{int_i}(\vec{\rho}_i) + V_{ext_i}(\vec{\rho}_i)$. The index α_i represents the quantum numbers describing the internal eigenfunctions ϕ_{α_i} and eigenenergies ε_{α_i} of the hamiltonian \hat{h}_i of the individual particle i . As an example, if we consider a diatomic molecule with no spin structure where $V_{int_i}(\vec{\rho}_i)$ represents the vibrational and rotational internal potential energy and if we consider no external potential energy $V_{ext_i} = 0$, then $\phi_{\alpha_i}(\vec{\rho}_i) = \frac{\chi_{v_i, n_i}(\rho_i)}{\rho_i} Y_{n_i}^{m_{n_i}}(\hat{\rho}_i)$. We note \hat{n}_i the rotational angular momentum operator of the molecule i characterized by the quantum number n_i , and \hat{n}_{Z_i} represents the projection operator of \hat{n}_i onto the OZ space-fixed frame axis characterized by the quantum numbers m_{n_i} . Then $Y_{n_i}^{m_{n_i}}(\hat{\rho}_i)$ represents the rotational wavefunction

where $\hat{\rho}_i$ represents the spherical angles of $\vec{\rho}_i$. Small hats corresponds to angles here, not to mistake with the wide hats of the quantum operators. χ_{v_i, n_i} represents the radial vibrational wavefunction characterized by the vibrational and rotational quantum numbers v_i, n_i . The quantum numbers describing the internal state are $\alpha_i \equiv v_i, n_i, m_{n_i}$. We note $\varepsilon_\alpha = \varepsilon_{\alpha_1} + \varepsilon_{\alpha_2}$, $\phi_\alpha = \phi_{\alpha_1} \phi_{\alpha_2}$, with $\alpha \equiv \alpha_1 \alpha_2$. The total energy of the system $E_{tot} = E_{k1} + E_{k2} + \varepsilon_\alpha$, where E_{ki} is the kinetic energy of particle i and is conserved during the collision. Because we consider potentials that do not depend on the individual position of the molecules, one can separate the center-of-mass with the relative coordinates, and we can write the wavefunction as a product $\psi(\vec{\rho}_1, \vec{\rho}_2, \vec{r}_1, \vec{r}_2) = \psi_{CM}(\vec{R}) \psi_{rel}(\vec{\rho}_1, \vec{\rho}_2, \vec{r})$. One can show that Eq. (10) can be decoupled into an equation for the center-of-mass motion:

$$\left[-\frac{\hbar^2}{2m_{tot}} \vec{\nabla}_{\vec{R}}^2 \right] \psi_{CM}(\vec{R}) = E_{kCM} \psi_{CM}(\vec{R}) \quad (12)$$

and one for the relative motion:

$$\begin{aligned} \left[-\frac{\hbar^2}{2m_{red}} \vec{\nabla}_{\vec{r}}^2 + U_{int}(\vec{\rho}_1, \vec{\rho}_2, \vec{r}) + \hat{h}_1(\vec{\rho}_1) + \hat{h}_2(\vec{\rho}_2) \right] \psi_{rel}(\vec{\rho}_1, \vec{\rho}_2, \vec{r}) \\ = (E_{tot} - E_{kCM}) \psi_{rel}(\vec{\rho}_1, \vec{\rho}_2, \vec{r}). \end{aligned} \quad (13)$$

with $E_{k1} + E_{k2} = E_{kCM} + E_{krel}$. For the type of separable interaction potential energy $U_{int}(\vec{\rho}_1, \vec{\rho}_2, \vec{r})$, the solution in Eq. (12) for the CM motion is a free motion unaffected by the internal interactions, and is represented as a plane wave. It can be separated from the collision problem. In the following, we consider the collision in the space-fixed frame $OXYZ$ of the center-of-mass so that $\vec{R} = 0$, $E_{kCM} = 0$, $E_{krel} = E_k$, and $E_{tot} = E_k + \varepsilon_\alpha$. Then Eq. (13) describes the motion of a fictitious particle of mass m_{red} , of internal state $\phi_\alpha = \phi_{\alpha_1} \phi_{\alpha_2}$ moving in the interacting potential $U_{int}(\vec{\rho}_1, \vec{\rho}_2, \vec{r})$. For simplicity we will omit the subscript ‘rel’ in the wavefunction.

2.2.2 Types of collisions

Fig. 2 shows different types of collisions, according to the different internal energy levels ε_α of the pair of particles, before the collision (left) and after the collision (right). For this example, there are five different possible states labeled $\alpha = 1, 2, 3, 4, 5$, with corresponding energies.

- (a) On the left-hand side of the figure, the initial internal level is $\alpha = 2$ and the initial internal energy ε^i is ε_2 (the superscript ‘i’ stands for ‘initial’ here).
- (b) The initial kinetic energy E_k^i is fixed and is called the **collision energy** E_c .
- (c) The total energy is $E_{tot} = \varepsilon^i + E_k^i$.
- (d) The states with an internal energy larger than the total energy are called the **closed states**, which are not energetically accessible after the collision.
- (e) The states with an internal energy smaller than the total energy are called the **open states** which are energetically accessible after the collision.

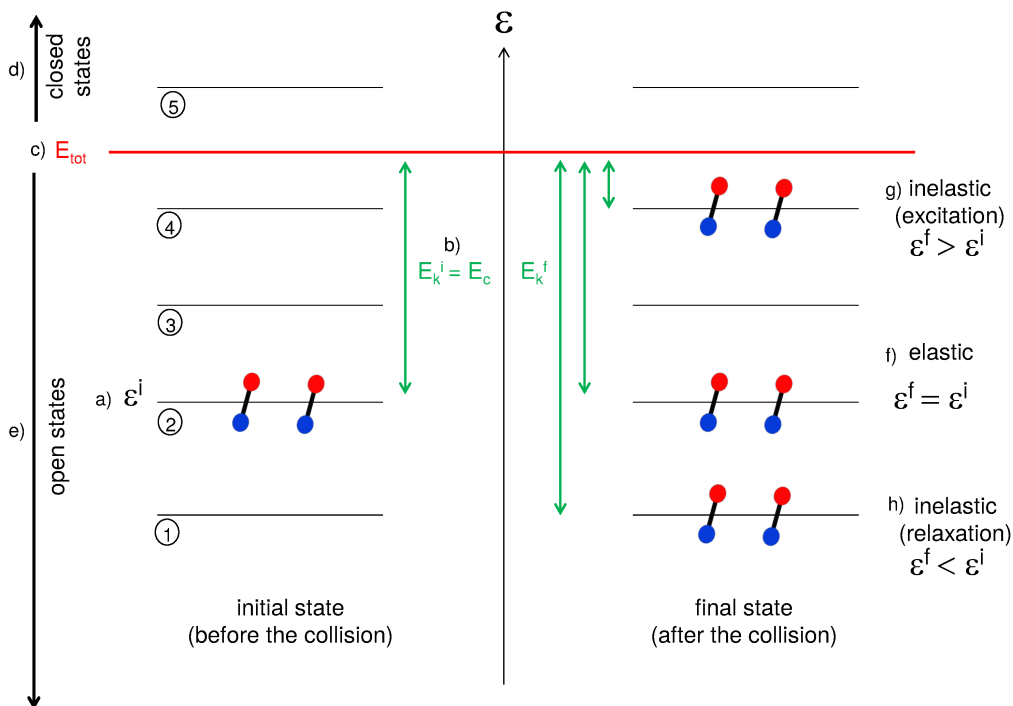


Figure 2: Sketch of the energy thresholds of two particles (here two diatomic molecules) when they are far from each other. The total energy E_{tot} is indicated as a red line and is conserved during a collision. It separates the open states from the closed states. The result of different types of collision is shown. For elastic collisions, the energy of the molecules is the same before and after the collision while for inelastic collisions, the energy is different. For excitation (relaxation) processes, the energy of the molecules has increased (decreased) so that their relative kinetic energy should decrease (increase) to conserve the total energy (see text for details).

- (f) An **elastic collision** occurs when the final state is the same as the initial one, $\varepsilon^f = \varepsilon^i$ (the superscript ‘f’ stands for ‘final’ here). As the total energy is conserved, the final kinetic energy $E_k^f = E_k^i$ is also conserved. When the particles have the same internal energy after and before the collision, they also have the same kinetic energy.
- (g) If the final state is different than the initial one ($\varepsilon^f \neq \varepsilon^i$), an **inelastic collision** takes place. The case $\varepsilon^f > \varepsilon^i$ corresponds to an **excitation** where $E_k^f < E_k^i$, leading to $E_k^f = E_{tot} - \varepsilon^f = \varepsilon^i - \varepsilon^f + E_k^i$. In this case, the particles have gained internal energy and lost kinetic energy.
- (h) The case $\varepsilon^f < \varepsilon^i$ refers to a **relaxation** with $E_k^f > E_k^i$, and $E_k^f = \varepsilon^i - \varepsilon^f + E_k^i$. In this case, the particles have lost internal energy and gained kinetic energy.

When the chemical identity of the products is different from the one of the reactants, various kinds of **reactive collisions** can occur providing that the states of the

products are open:

$$\begin{aligned}
AB + CD &\rightarrow AC + BD, AD + BC \\
&\rightarrow A + BCD, B + CDA, C + DAB, D + ABC \\
&\rightarrow A + B + CD, B + C + DA, \\
&\quad C + D + AB, D + A + BC \\
&\rightarrow A + B + C + D.
\end{aligned}$$

In such cases, a set of collective coordinates like the so-called hyperspherical coordinates [56, 57] should be employed as they are more appropriate than the Jacobi coordinates to treat the different arrangements or the four particles in a more symmetric way. The resulting collisional formalism is more complicated [58, 59, 60] and beyond the scope of this paper. Therefore we will not treat the case of reactive collisions in the following, only the case of elastic and inelastic collisions.

3 In the region far from collision

3.1 Asymptotic form of the wavefunction

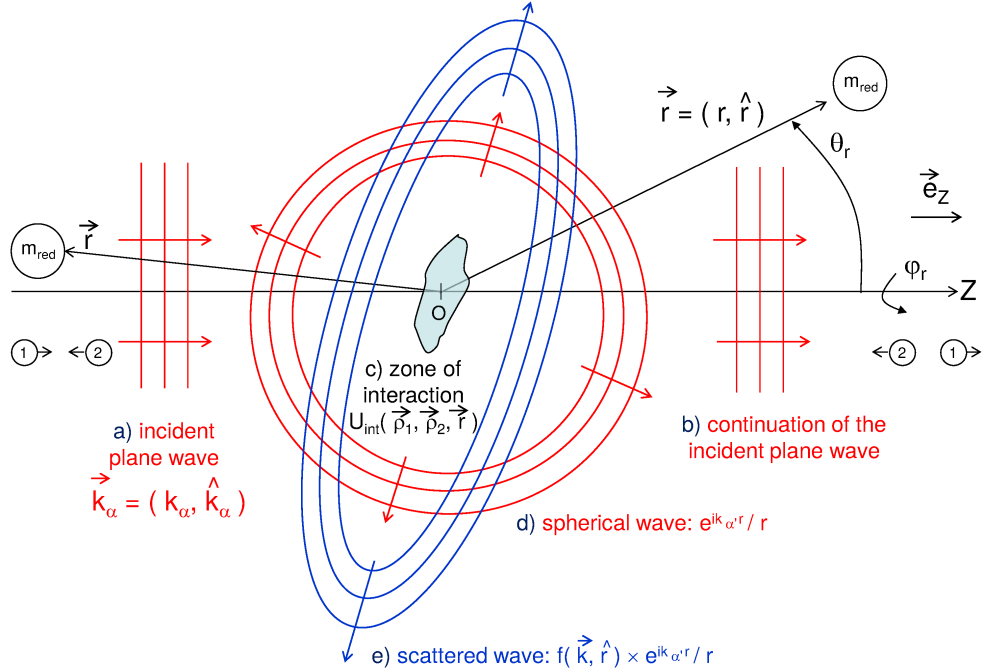


Figure 3: Asymptotic form of the total wavefunction which decomposes into a incident plane wave and a scattered wave due to the effect of the interaction U_{int} (see text for details).

As mentioned above, the motion of the center-of-mass can be separated from the collision problem. We then don't consider it anymore and we focus now on the relative motion described by the fictitious particle of mass m_{red} . The relative vector \vec{r} can be written in spherical coordinates $\vec{r} = \{r, \hat{r} = (\theta_r, \varphi_r)\}$ with respect to the OZ space-fixed frame axis. The stationary scattering state for the relative motion in the CM frame for a given total energy E_{tot} and for an initial state α, \vec{k}_α behaves asymptotically as:

$$\begin{aligned} \psi_{\alpha, \vec{k}_\alpha}^{E_{tot}}(\vec{\rho}_1, \vec{\rho}_2, \vec{r}) &\underset{r \rightarrow \infty}{=} \mathcal{A} \left[e^{i\vec{k}_\alpha \cdot \vec{r}} \phi_\alpha(\vec{\rho}_1, \vec{\rho}_2) \right. \\ &\quad \left. + \sum_{\alpha'} f_{\alpha \rightarrow \alpha'}^+(\vec{k}_\alpha, \hat{r}) \frac{e^{ik_{\alpha'} r}}{r} \phi_{\alpha'}(\vec{\rho}_1, \vec{\rho}_2) \right] \quad (14) \\ &= \psi_{inc} + \psi_{scat}. \end{aligned}$$

\mathcal{A} is a normalization factor which does not play a role for the result of the collision as we will see later. One could set $\mathcal{A} = 1$ for simplicity. Fig. 3 represents schematically the asymptotic form of the wavefunction and is separated in different parts:

- (a) The incident wavefunction ψ_{inc} is composed of an initial incident plane wave $e^{i\vec{k}_\alpha \cdot \vec{r}}$ and the internal structure of the particles $\phi_\alpha(\vec{\rho}_1, \vec{\rho}_2)$. ψ_{inc} is a solution of Eq. (13) when $U_{int} \rightarrow 0$ at $r \rightarrow \infty$. The plane wave is characterized by a wavevector \vec{k}_α of magnitude k_α and incident direction \hat{k}_α . The initial kinetic energy is $E_{k,\alpha} = \hbar^2 k_\alpha^2 / 2m_{red} = E_c$. In general \vec{k}_α can take any orientation with respect to \vec{e}_Z . In Fig.3, \vec{k}_α has been chosen with the same orientation than \vec{e}_Z . The incident wavefunction ψ_{inc} is expressed as a plane wave describing the particles at $Z \rightarrow -\infty$. A part of the plane wave may continue to propagate towards $Z \rightarrow +\infty$ without interacting in the potential range.
- (b) In the zone of interaction around $Z \sim 0$, the particles interact via the interaction potential energy $U_{int}(\vec{\rho}_1, \vec{\rho}_2, \vec{r})$.
- (c) Due to this interaction, the plane wave can also be scattered in a spherical manner. This is represented by a spherical wave $e^{ik_{\alpha'} r} / r$.
- (d) Due to the specific shape of the interaction potential, the plane wave is scattered with an amplitude $f_{\alpha \rightarrow \alpha'}^+(\vec{k}_\alpha, \hat{r})$, referred to as the **scattering amplitude**. It represents the probability amplitude of the two particles for being scattered in the direction \hat{r} from the initial state α with wavevector \vec{k}_α into the final state α' . ψ_{scat} represents the overall scattered wavefunction including the internal structure.

3.2 Observables

We relate now the scattering amplitude to the observables. Considering a typical beam/target collision experiment, the observable is the number of the beam particles, say particles 1, scattered out of the target particles, say particles 2, per unit of time and solid angle and detected by a detector in the laboratory frame somewhere far from the region of collision. In the CM frame it translates into the the number of fictitious particles of mass m_{red} scattered out of the potential per unit of time and of

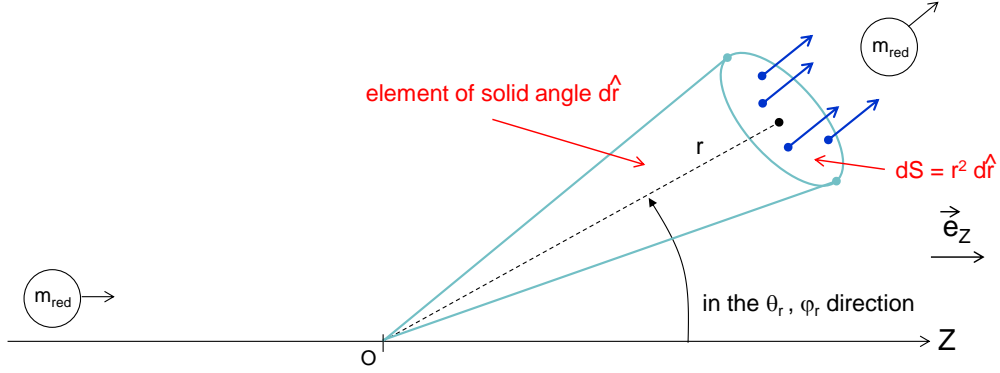


Figure 4: Flux of fictive particles of mass m_{red} into a detector far from the collision region.

solid angle $d\hat{r} = \sin\theta_r d\theta_r d\varphi_r$, detected by the detector in the direction $\hat{r} = (\theta_r, \varphi_r)$ for a transition $\alpha \rightarrow \alpha'$, and for a given incident direction \vec{k}_α (see Fig. 4). This number is proportional to the incident probability current $J_{inc} = N_{inc} j_{inc}$ of the N_{inc} incoming particles of mass m_{red} . This is given by:

$$\left. \frac{\partial N_{scat}}{\partial t \partial \hat{r} \partial \hat{k}_\alpha}(\vec{k}_\alpha, \hat{r}) \right|_{\alpha \rightarrow \alpha'} = J_{inc} \frac{\partial \sigma_{\alpha \rightarrow \alpha'}(\vec{k}_\alpha, \hat{r})}{\partial \hat{r} \partial \hat{k}_\alpha}. \quad (15)$$

The quantity $\frac{\partial \sigma(\vec{k}_\alpha, \hat{r})}{\partial \hat{r} \partial \hat{k}_\alpha}$ is called the **differential cross section**. The flux of J_{inc} in the differential cross section gives the number of particles scattered per unit of time and solid angle. By expressing j_{inc} and j_{scat} from ψ_{inc} and ψ_{scat} in Eq. (14), using the first line of the time-independent version of Eq. (3), one can show that:

$$\frac{\partial \sigma_{\alpha \rightarrow \alpha'}(\vec{k}_\alpha, \hat{r})}{\partial \hat{r} \partial \hat{k}_\alpha} = \frac{k_{\alpha'}}{k_\alpha} |f_{\alpha \rightarrow \alpha'}^+(\vec{k}_\alpha, \hat{r})|^2. \quad (16)$$

The **integral cross section** for a given direction \vec{k}_α of collision is given by integrating the differential cross section over all scattering directions:

$$\sigma_{\alpha \rightarrow \alpha'}(\vec{k}_\alpha) = \int \frac{\partial \sigma(\vec{k}_\alpha, \hat{r})}{\partial \hat{r} \partial \hat{k}_\alpha} d\hat{r} = \frac{k_{\alpha'}}{k_\alpha} \int |f_{\alpha \rightarrow \alpha'}^+(\vec{k}_\alpha, \hat{r})|^2 d\hat{r}. \quad (17)$$

If the direction of collision is not specified (for example in a gas-cell experiment in contrast to a beam experiment), one also has to average over the value of the incident directions to obtain the averaged integral cross section for a given collision energy $E_c = \hbar^2 k_\alpha^2 / 2m_{red}$:

$$\sigma_{\alpha \rightarrow \alpha'}(k_\alpha) = \sigma_{\alpha \rightarrow \alpha'}(E_c) = \frac{\int \sigma_{\alpha \rightarrow \alpha'}(\vec{k}_\alpha) d\hat{k}_\alpha}{\int d\hat{k}_\alpha} = \frac{1}{4\pi} \int \sigma_{\alpha \rightarrow \alpha'}(\vec{k}_\alpha) d\hat{k}_\alpha. \quad (18)$$

Because:

$$\left. \frac{\partial N_{scat}}{\partial t} \right|_{\alpha \rightarrow \alpha'} = \frac{1}{4\pi} \int d\hat{k}_\alpha \int d\hat{r} \left. \frac{\partial N_{scat}}{\partial t \partial \hat{r} \partial \hat{k}_\alpha}(\vec{k}_\alpha, \hat{r}) \right|_{\alpha \rightarrow \alpha'} = J_{inc} \times \sigma_{\alpha \rightarrow \alpha'}(E_c), \quad (19)$$

we see that the number of scattered particles per unit of time, summed over all incident directions is the flux of the incident probability current J_{inc} through the averaged integral cross section $\sigma_{\alpha \rightarrow \alpha'}(E_c)$. Then because $J_{inc} = N_{inc}/\Delta S \Delta t$ is the number of incident particles crossing a given surface ΔS in the time interval Δt , $N_{scat}/N_{inc} = \sigma/\Delta S$. Choosing a unit surface $\Delta S = 1 \text{ cm}^2$, σ expressed in cm^2 represents the number of scattered particles relative to the number of incident particles. For gas-cell experiments, one usually has access to the initial volumic density ρ_{gas} of the gas, not to the initial current J_{inc} . Using the second line of the time-independent version of Eq. (3) and applying it to ψ_{inc} in Eq. (14), one can notice that $j_{inc} = |\psi_{inc}|^2 v = \rho_{inc} v$, where $v = \hbar k_\alpha / m_{red} = \sqrt{2E_c/m_{red}}$ is the initial velocity of the fictitious particle, that is the relative initial velocity of the two colliding particles. Then $J_{inc} = (N_{inc} \rho_{inc}) v = \rho_{gas} v$. If we define another observable:

$$\beta_{\alpha \rightarrow \alpha'}(E_c) = \sigma_{\alpha \rightarrow \alpha'}(E_c) \times v, \quad (20)$$

called the **rate coefficient**, then Eq. (19) becomes now:

$$\left. \frac{\partial N_{scat}}{\partial t} \right|_{\alpha \rightarrow \alpha'} = \rho_{gas} \times \beta_{\alpha \rightarrow \alpha'}(E_c). \quad (21)$$

Therefore by knowing the initial volumic density instead of the the initial current, one extracts directly the rate coefficients instead of the cross sections, from the number of particles scattered per unit of time. If the cross section has unit of cm^2 and the velocity has unit of cm/s , the rate coefficient has unit of cm^3/s .

4 In the region of collision

So far we have just defined some relevant quantities for the collisional properties of a system. We are now interested in how to calculate the cross section and the rate coefficient from a given potential energy.

4.1 Partial wave expansion

In Eq. (14), the plane wave appearing in ψ_{inc} is a function of the vector \vec{r} . When \vec{r} is represented by spherical coordinates $\vec{r} = \{r, \hat{r} = (\theta_r, \varphi_r)\}$, the kinetic energy operator in Eq. (13) can be expressed in spherical coordinates by:

$$-\frac{\hbar^2}{2m_{red}} \vec{\nabla}_{\vec{r}}^2 \equiv -\frac{\hbar^2}{2m_{red}} \left[\frac{1}{r^2} \frac{\partial}{\partial r} \left(r^2 \frac{\partial}{\partial r} \right) \right] + \frac{\hat{l}^2}{2m_{red} r^2}, \quad (22)$$

The spherical harmonics $Y_l^{m_l}(\hat{r})$ are eigenfunctions of the square of the angular momentum operator \hat{l}^2 so that $\hat{l}^2 Y_l^{m_l} = \hbar^2 l(l+1) Y_l^{m_l}$. Using the spherical harmonic addition theorem, the plane wave in Eq. (14) can be expanded in spherical harmonics of quantum numbers l, m_l :

$$\begin{aligned} \psi_{inc} &= \mathcal{A} e^{i\vec{k}_\alpha \cdot \vec{r}} \phi_\alpha(\vec{\rho}_1, \vec{\rho}_2) \\ &= \mathcal{A} 4\pi \sum_{l=0}^{\infty} \sum_{m_l=-l}^l i^l j_l(k_\alpha r) [Y_l^{m_l}(\hat{k}_\alpha)]^* Y_l^{m_l}(\hat{r}) \phi_\alpha(\vec{\rho}_1, \vec{\rho}_2). \end{aligned} \quad (23)$$

j_l is a regular spherical Bessel function which behaves at large distances as:

$$\begin{aligned} j_l(k_\alpha r) &\xrightarrow{r \rightarrow \infty} \frac{\sin(k_\alpha r - l\pi/2)}{k_\alpha r} \\ &\rightarrow \frac{i}{2k_\alpha r} \left[e^{-i(k_\alpha r - l\pi/2)} - e^{i(k_\alpha r - l\pi/2)} \right]. \end{aligned} \quad (24)$$

The asymptotic behavior of ψ_{inc} is then:

$$\psi_{inc} \xrightarrow{r \rightarrow \infty} \sum_{l=0}^{\infty} \sum_{m_l=-l}^l N_{\alpha l m_l}^{inc}(\vec{k}_\alpha) \psi_{\alpha l m_l}^{inc}(\vec{\rho}_1, \vec{\rho}_2, \vec{r}), \quad (25)$$

where $N_{\alpha l m_l}^{inc}(\vec{k}_\alpha) \equiv \mathcal{A}(2\pi i)/k_\alpha^{1/2} i^l [Y_l^{m_l}(\hat{k}_\alpha)]^*$ is a normalization factor independent of r . The functions:

$$\psi_{\alpha l m_l}^{inc}(\vec{\rho}_1, \vec{\rho}_2, \vec{r}) \equiv \frac{f^{inc}(r)}{r} Y_l^{m_l}(\hat{r}) \phi_\alpha(\vec{\rho}_1, \vec{\rho}_2) \quad (26)$$

are called the **partial waves**, where $f^{inc}(r) = (e^{-i(k_\alpha r - l\pi/2)} - e^{i(k_\alpha r - l\pi/2)})/k_\alpha^{1/2}$ is the incident radial function (not to be mistaken with the scattering amplitude f^+). The expansion over the quantum numbers l, m_l is called the partial wave expansion which represents the description of the colliding system in terms of components of the orbital angular momentum of the translational (collisional) motion. We then extend to all r the partial wave expansion Eq. (25) for the total wavefunction $\psi_{\alpha, \vec{k}_\alpha}^{E_{tot}}$, for a given total energy E_{tot} , an initial internal quantum state of the molecules α and an initial wavevector \vec{k}_α :

$$\psi_{\alpha, \vec{k}_\alpha}^{E_{tot}}(\vec{\rho}_1, \vec{\rho}_2, \vec{r}) = \sum_{l=0}^{\infty} \sum_{m_l=-l}^l N_{\alpha l m_l}(\vec{k}_\alpha) \psi_{\alpha l m_l}^{E_{tot}}(\vec{\rho}_1, \vec{\rho}_2, \vec{r}), \quad (27)$$

where $N_{\alpha l m_l}(\vec{k}_\alpha)$ is the normalization factor for the wavefunction $\psi_{\alpha l m_l}^{E_{tot}}$. It will be defined, in Eq. (69), by matching $\psi^{E_{tot}}$ to the asymptotic form of the wavefunction. At finite r , the partial waves in Eq. (26) are now expressed by:

$$\psi_{\alpha l m_l}^{E_{tot}}(\vec{\rho}_1, \vec{\rho}_2, \vec{r}) = \sum_{\alpha'} \sum_{l'=0}^{\infty} \sum_{m'_l=-l'}^{l'} \frac{f_{\alpha' l' m'_l, \alpha l m_l}^{E_{tot}}(r)}{r} Y_{l'}^{m'_l}(\hat{r}) \phi_{\alpha'}(\vec{\rho}_1, \vec{\rho}_2). \quad (28)$$

In contrast with Eq. (26) for the incident wavefunction, we now allow in Eq. (28) the components $\psi_{\alpha l m_l}^{E_{tot}}(\vec{\rho}_1, \vec{\rho}_2, \vec{r})$ to be a general, linear combination of the other final internal states α' and final orbital quantum numbers l', m'_l . This is due to the presence at finite r of the potential energy term which can couple the initial state to all the other final states. The quantum numbers $(\alpha l m_l)$ and $(\alpha' l' m'_l)$ define the **collisional channels** for the initial and final states, respectively. The functions $f_{\alpha' l' m'_l, \alpha l m_l}^{E_{tot}}$ will be responsible for the transitions $\alpha l m_l \rightarrow \alpha' l' m'_l$. The transition is inelastic if $\alpha \neq \alpha'$ or elastic if $\alpha = \alpha'$ as illustrated in Fig. 2. In Eq. (28), one can define the **basis set functions**:

$$\Phi_{\alpha' l' m'_l}(\vec{\rho}_1, \vec{\rho}_2, \hat{r}) \equiv Y_{l'}^{m'_l}(\hat{r}) \phi_{\alpha'}(\vec{\rho}_1, \vec{\rho}_2) \quad (29)$$

which include all but the radial colliding motion degrees of freedom. If we take the example mentioned above of two diatomic molecules with no spin, this basis set is:

$$\Phi_{\alpha' l' m'_l}(\vec{\rho}_1, \vec{\rho}_2, \hat{r}) = \frac{\chi_{v'_1, n'_1}(\rho_1)}{\rho_1} \frac{\chi_{v'_2, n'_2}(\rho_2)}{\rho_2} Y_{n'_1}^{m'_1}(\hat{\rho}_1) Y_{n'_2}^{m'_2}(\hat{\rho}_2) Y_{l'}^{m'_l}(\hat{r}). \quad (30)$$

The basis set in Eq. (29) is independent of the particles separation r , referred to as a **diabatic representation**. There are other possible representations, such as the **diabatic-by-sector representation** or the **adiabatic representation** which involves additional coupling terms. Such cases are beyond the scope of this paper. Note that the formalism chosen here uses coordinate axes that point in the space-fixed frame directions, in particular the quantization axis is oriented along the space-fixed unit vector \vec{e}_Z . For that reason, this is referred to a **space-fixed frame formalism** [62, 63, 64, 65, 66]. In contrast, there is also a **body-fixed frame formalism** [61, 64, 67, 66, 68] where the coordinate axes follow the body-fixed axes (see Fig. 1). The two formulations are equivalent. The appropriate formalism depends on the treated problem. Generally, it is more efficient to use the space-fixed frame approach for large J , long range, weak coupling collisions, and the body-fixed frame approach for small J , short range, strong coupling collisions [64]. Finally, because the basis set in Eq. (29) uses uncoupled functions of angular momentum, this is called the **uncoupled representation** of the wavefunction [61, 62]. In contrast, one can use a **coupled representation** [61, 62, 63, 69, 70, 65, 66] where all composite functions of angular momentum are coupled together to form a total angular momentum. Taking as example the basis set of a diatomic molecule in Eq. (30), one can couple their rotational angular momenta operators \hat{n}_1 and \hat{n}_2 and projections \hat{n}_{Z_1} and \hat{n}_{Z_2} , into a coupled rotational angular momentum operator \hat{n}_{12} and projection $\hat{n}_{Z_{12}}$ with characteristic quantum numbers $n_{12}, m_{n_{12}}$. The coupled rotational wavefunction becomes:

$$Y_{n_{12}}^{m_{n_{12}}} = \sum_{m_{n_1}, m_{n_2}} \langle n_1, m_{n_1}, n_2, m_{n_2} | n_{12}, m_{n_{12}} \rangle Y_{n_1}^{m_{n_1}}(\hat{\rho}_1) Y_{n_2}^{m_{n_2}}(\hat{\rho}_2). \quad (31)$$

The coupled rotational angular momentum operator \hat{n}_{12} and orbital angular momentum \hat{l} , and projections $\hat{n}_{Z_{12}}$ and \hat{l}_Z , can be further coupled to form the total angular momentum operator \hat{J} and projection \hat{J}_Z with characteristic quantum numbers J, M_J . The fully coupled wavefunction becomes:

$$Y_J^{M_J} = \sum_{m_{n_{12}}, m_l} \langle n_{12}, m_{n_{12}}, l, m_l | J, M_J \rangle Y_{n_{12}}^{m_{n_{12}}} Y_l^{m_l}(\hat{r}) \quad (32)$$

with $M_J = m_{n_{12}} + m_l = m_{n_1} + m_{n_2} + m_l$. The basis set is completed by combining this angular basis set with the internal radial functions $\frac{\chi_{v_1, n_1}(\rho_1)}{\rho_1} \frac{\chi_{v_2, n_2}(\rho_2)}{\rho_2}$. The quantum numbers describing the wavefunction in the coupled representation are now $v_1, v_2, n_1, n_2, n_{12}, l, J, M_J$ in contrast with $v_1, v_2, n_1, m_{n_1}, n_2, m_{n_2}, l, m_l$ for the uncoupled representation. If the total potential energy satisfies $V(-\vec{\rho}_1, -\vec{\rho}_2, -\vec{r}) = V(\vec{\rho}_1, \vec{\rho}_2, \vec{r})$, then J and M_J are good quantum numbers and are conserved during the collision. This is the case when no external potentials V_{ext} are applied, as the

potential energy surface V_{int} does not depend on the global orientation of the two particles. Then when no external field is applied it is useful to use the coupled representation since J and M_J are good quantum numbers, which leads to efficient and fast numerical calculations. When external potentials V_{ext} are applied, such as with arbitrary external electric or magnetic fields, different states with different values of J become coupled so that J is no more a good quantum number. Therefore the coupled representation loses its advantage. In contrast M_J is still conserved if only one of the electric or the magnetic field is present at a time or if both fields share the same quantization axis. Once both fields are not aligned [71], M_J is not a good quantum number anymore. To treat ultracold collisions in any arbitrary external fields, including both weak and strong regimes, the uncoupled representation is generally preferred. The weak (strong) regime corresponds respectively to an interaction between the particle and the field much smaller (bigger) than the typical zero-field particle energy. For example for a diatomic molecule with a permanent electric dipole moment d , one has to compare the magnitude dE of the interaction of the molecule with an electric field E , with its typical energy without field, that is the rotational constant of the molecule B_{rot} . The weak (strong) regime is reached when typically $dE \ll B_{rot}$ ($dE \gg B_{rot}$). Note though that in case of strongly dominated anisotropic collisions [72, 73] the use of a body-fixed coupled representation can still be beneficial for efficient calculations, provided an appropriate treatment of unphysical states. In the following, we will use the uncoupled representation in the collisional formalism since it is more intuitive to think in term of the individual quantum numbers of the separated particles. Besides, the last section of the paper will illustrate the case of dipolar molecules collisions in an electric field where the uncoupled representation is preferred and where the following formalism applies.

4.2 Coupled equations

We look now for the equations satisfied by the radial functions in Eq. (28). The Schrödinger equation for a given partial wave l, m_l is:

$$\hat{H} \psi_{\alpha l m_l}^{E_{tot}} = E_{tot} \psi_{\alpha l m_l}^{E_{tot}} \quad (33)$$

with $E_{tot} = \varepsilon_{\alpha} + \frac{\hbar^2 k_{\alpha}^2}{2m_{red}} = \varepsilon_{\alpha} + E_c$ and \hat{H} given in Eq. (13). Inserting Eq. (28) into Eq. (33) and using Eq. (22), we obtain:

$$\sum_{\alpha'} \sum_{l'=0}^{\infty} \sum_{m'_l=-l'}^{l'} \left[-\frac{\hbar^2}{2m_{red}} \frac{d^2}{dr^2} + \frac{\hbar^2 l'(l'+1)}{2m_{red} r^2} + U_{int}(\vec{\rho}_1, \vec{\rho}_2, \vec{r}) + \varepsilon_{\alpha'} - E_{tot} \right] \times f_{\alpha' l' m'_l, \alpha l m_l}^{E_{tot}}(r) Y_{l'}^{m'_l}(\hat{r}) \phi_{\alpha'}(\vec{\rho}_1, \vec{\rho}_2) = 0. \quad (34)$$

The first derivatives and the $1/r$ term have disappeared in Eq. (34) due to the choice of the form $f(r)/r$ in Eq. (28). If we multiply the left-hand side of Eq. (34) by $[Y_{l'}^{m'_l}(\hat{r})]^* \phi_{\alpha'}^*(\vec{\rho}_1, \vec{\rho}_2)$ and integrate over all but the radial coordinate r , we are led

to a system of coupled equations:

$$\sum_{\alpha'} \sum_{l'=0}^{\infty} \sum_{m'_l=-l'}^{l'} \left[\left\{ -\frac{\hbar^2}{2m_{red}} \frac{d^2}{dr^2} + \frac{\hbar^2 l'(l'+1)}{2m_{red}r^2} + \varepsilon_{\alpha'} - E_{tot} \right\} \delta_{\alpha',\alpha''} \delta_{l',l''} \delta_{m'_l,m''_l} \right. \\ \left. + \mathcal{U}_{\alpha'' l'' m''_l, \alpha' l' m'_l}^{int}(r) \right] f_{\alpha' l' m'_l, \alpha l m_l}^{E_{tot}}(r) = 0, \quad (35)$$

where:

$$\mathcal{U}_{\alpha'' l'' m''_l, \alpha' l' m'_l}^{int}(r) = \\ \int d\vec{\rho}_1 d\vec{\rho}_2 d\hat{r} [Y_{l''}^{m''_l}(\hat{r})]^* \phi_{\alpha''}^*(\vec{\rho}_1, \vec{\rho}_2) U_{int}(\vec{\rho}_1, \vec{\rho}_2, \vec{r}) Y_{l'}^{m'_l}(\hat{r}) \phi_{\alpha'}(\vec{\rho}_1, \vec{\rho}_2) \\ = \int d\vec{\rho}_1 d\vec{\rho}_2 d\hat{r} \Phi_{\alpha'' l'' m''_l}^*(\vec{\rho}_1, \vec{\rho}_2, \hat{r}) U_{int}(\vec{\rho}_1, \vec{\rho}_2, \vec{r}) \Phi_{\alpha' l' m'_l}(\vec{\rho}_1, \vec{\rho}_2, \hat{r}) \quad (36)$$

is a matrix element of the **coupling matrix** \mathcal{U}^{int} . This matrix is real, symmetric and in general non-diagonal. It provides the couplings between the collisional channel $\alpha'' l'' m''_l$ to $\alpha' l' m'_l$ and is responsible for the inelastic transition in the collision. There are as many line equations of Eq. (35) as there are $\alpha'' l'' m''_l$ numbers. All but the translational radial motion r , including the vibration and rotation of the molecules and the orbital angular momentum of the collision, has been integrated out in Eq. (36). This provides a set of second-order coupled differential equations for the radial functions $f_{\alpha' l' m'_l, \alpha l m_l}^{E_{tot}}(r)$ for a given $\alpha l m_l$ and E_{tot} . A **centrifugal term** has appeared in Eq. (34) and Eq. (35) coming from the development of the kinetic energy operator into an angular term proportional to the operator \widehat{l}^2 . One can define the corresponding (diagonal) matrix \mathcal{U}^{cent} with (diagonal) matrix elements:

$$\mathcal{U}_{\alpha'' l'' m''_l, \alpha' l' m'_l}^{cent}(r) = \frac{\hbar^2 l'(l'+1)}{2m_{red}r^2} \delta_{\alpha',\alpha''} \delta_{l',l''} \delta_{m'_l,m''_l}. \quad (37)$$

At ultralow collision energy, only a few, low quantum numbers of l are required to describe the collision in Eq. (35) since higher values of l implies higher values of the centrifugal barrier elements. Then this will imply lower values of the tunneling probability, which prevents the particles to come close to each other as $E_c \rightarrow 0$. As more values of l are required for higher E_c , the time-independent partial wave method is more adapted to study collision at ultralow energies than at high energies.

It is often useful to plot some elements of the set of equations to get a knowledge of how strong the system is coupled. Defining the indexes $i'' \equiv \alpha'' l'' m''_l$ and $i' \equiv \alpha' l' m'_l$, one can extract an effective potential matrix \mathcal{U}^{eff} in Eq. (35) with the following matrix elements:

$$\mathcal{U}_{i'',i'}^{eff}(r) = \mathcal{U}_{i'',i'}^{cent}(r) + \mathcal{U}_{i'',i'}^{int}(r) + \varepsilon_{\alpha'} \delta_{i',i''}, \quad (38)$$

which includes the diagonal centrifugal term elements, the coupling matrix elements and the energy thresholds of the two particles. One can plot each diagonal element

of this matrix as a function of r . The corresponding curves are called **the diabatic energy curves** and each of them tend at large r to one of the threshold energies of the two particles. These curves provide a set of all possible effective potentials for the radial motion of the two colliding particles, when the non-diagonal terms of the coupling matrix are not present. One can also include the effects of the non-diagonal terms of the coupling matrix in Eq. (38) by diagonalizing first the matrix \mathcal{U}^{eff} and then plot the eigenvalues as a function of r . The resulting curves are called **the adiabatic energy curves**, each of them tend as well to the threshold energies of the two particles at large r . These curves also provide a set of effective potentials for the radial motion, but now when the effect of the couplings is present. When comparing both types of curves, one can see directly how and where the non-diagonal couplings elements affect the diagonal elements. If the adiabatic curves are quite comparable to the diabatic curves, then the system is weakly coupled. However, it is strongly coupled if both types of curves differ significantly. This is illustrated later in the Section 7 in Fig. 7.

Finally, the system of coupled equations can be expressed in a very compact form [74, 75, 76], using a matrix notation:

$$\left\{ \mathbf{D}^2 + \mathbf{W} \right\} \mathbf{F} = \mathbf{0}. \quad (39)$$

The matrix:

$$\mathbf{D}^2 = \mathbf{I} \frac{d^2}{dr^2} \quad (40)$$

is a diagonal matrix, \mathbf{I} being the identity matrix. \mathbf{W} and \mathbf{F} are real and symmetric matrices. The matrix elements of \mathbf{W} are:

$$W_{i'',i'} = -\frac{2m_{red}}{\hbar^2} \left[\mathcal{U}_{i'',i'}^{cent}(r) + \mathcal{U}_{i'',i'}^{int}(r) + (\varepsilon_{\alpha'} - E_{tot}) \delta_{i',i''} \right]. \quad (41)$$

The square matrix \mathbf{F} involves the radial functions, and its elements are given by $F_{i',i} = f_{i',i}^{E_{tot}}(r)$ for which the line $i' \equiv \alpha' l' m'_l$ refers to the final state and the column $i \equiv \alpha l m_l$ to the initial state. There are as many initial states as there are open channels for a given total energy E_{tot} . For example in Figure 2, there are 4 open channels at the given total energy, say $i = 1, 2, 3, 4$ with increasing energies $\varepsilon_1, \varepsilon_2, \varepsilon_3, \varepsilon_4$. The initial state is two molecules in $i = 2$ with internal energy ε_2 with a collision energy E_c and total energy $E_{tot} = \varepsilon_2 + E_c$. The solution of the wavefunction is the column $i = 2$ of \mathbf{F} . The other columns of \mathbf{F} represent the other independent solutions of the wavefunction corresponding to a total energy E_{tot} but different initial conditions: $i = 1$ corresponds to an initial state where the molecules start with internal energy ε_1 and collision energy $E_c = E_{tot} - \varepsilon_1$, $i = 3$ to ε_3 and $E_c = E_{tot} - \varepsilon_3$ and finally $i = 4$ to ε_4 and $E_c = E_{tot} - \varepsilon_4$. Each column of \mathbf{F} then represents a linearly independent solution of the problem.

4.3 Case of long-range interactions described by an electrostatic multipole-multipole expansion

In practical, one has to compute all the elements U^{int} of the coupling matrix in Eq. (36). This requires the knowledge of the full potential energy surface $U_{int}(\vec{\rho}_1, \vec{\rho}_2, \vec{r})$. At long-range, the potential energy surface can be described in terms of an electrostatic multipole-multipole expansion [77]:

$$U_{mult} = \frac{1}{4\pi\epsilon_0} \sum_{\lambda_1 \lambda_2} \sum_{\lambda \omega_{\lambda_1} \omega_{\lambda_2}} (-1)^{\lambda_1} \left(\frac{(2\lambda_1 + 2\lambda_2 + 1)!}{(2\lambda_1)!(2\lambda_2)!} \right)^{1/2} \frac{Q_{\lambda_1 \omega_{\lambda_1}} Q_{\lambda_2 \omega_{\lambda_2}}}{r^{\lambda+1}} \times \delta_{\lambda, \lambda_1 + \lambda_2} \sum_{m_{\lambda_1} m_{\lambda_2} m_{\lambda}} \mathcal{A}(\hat{\rho}_1, \hat{\rho}_2, \hat{r}) \quad (42)$$

with $\lambda = \lambda_1 + \lambda_2$. The angular part is given by:

$$\mathcal{A}(\hat{\rho}_1, \hat{\rho}_2, \hat{r}) = \begin{pmatrix} \lambda_1 & \lambda_2 & \lambda \\ m_{\lambda_1} & m_{\lambda_2} & -m_{\lambda} \end{pmatrix} \times [D_{m_{\lambda_1} \omega_{\lambda_1}}^{\lambda_1}(\hat{\rho}_1)]^* [D_{m_{\lambda_2} \omega_{\lambda_2}}^{\lambda_2}(\hat{\rho}_2)]^* [D_{-m_{\lambda} 0}^{\lambda}(\hat{r})]^*. \quad (43)$$

The symbol ($::$) is a Wigner 3-j symbol related to a Clebsch–Gordan coefficient and it is non-zero only if $m_{\lambda} = m_{\lambda_1} + m_{\lambda_2}$ and if $\lambda_1, \lambda_2, \lambda$ satisfy the triangle relation. $Q_{\lambda_i \omega_{\lambda_i}}$ is a generalized multipole in the body-fixed frame of the molecule where we choose the unit vector $\vec{\rho}_i/|\vec{\rho}_i|$ for molecule $i = 1, 2$ in Fig. 1 to characterize the quantization axis. λ_i is an angular momentum quantum number corresponding to the electronic charge distribution in the molecules $i = 1, 2$. $\lambda_i = 0, 1, 2, 3, \dots$ correspond respectively to the **charge, dipole, quadrupole, octopole moments**, and so on. $m_{\lambda_i} = [-\lambda_i, +\lambda_i]$ are the projection of these angular momenta onto the space-fixed frame quantization axis \vec{e}_Z . $\omega_{\lambda_i} = [-\lambda_i, +\lambda_i]$ is the projection onto the body-fixed frame quantization axis $\vec{\rho}_i/|\vec{\rho}_i|$ of molecule i . In the case of Σ electronic diatomic molecules, $\omega_{\lambda_1} = \omega_{\lambda_2} = 0$ and one can write Eq. (43) using the rotational eigenfunctions $|n_1, m_{n_1}\rangle$ and $|n_2, m_{n_2}\rangle$ of the molecules 1 and 2 for the internal wavefunction ϕ_{α} :

$$\begin{aligned} \langle n_1, m_{n_1}, n_2, m_{n_2}, l, m_l | U_{mult} | n'_1, m'_{n_1}, n'_2, m'_{n_2}, l', m'_l \rangle = & \\ \frac{1}{4\pi\epsilon_0} \sum_{\lambda_1 \lambda_2} (-1)^{\lambda_1} \left(\frac{(2\lambda_1 + 2\lambda_2 + 1)!}{(2\lambda_1)!(2\lambda_2)!} \right)^{1/2} \frac{Q_{\lambda_1 0} Q_{\lambda_2 0}}{r^{\lambda_1 + \lambda_2 + 1}} & \\ \sum_{m_{\lambda_1} m_{\lambda_2}} (-1)^{m_{n_1} + m_{n_2} + m_l} \begin{pmatrix} \lambda_1 & \lambda_2 & \lambda_1 + \lambda_2 \\ m_{\lambda_1} & m_{\lambda_2} & -(m_{\lambda_1} + m_{\lambda_2}) \end{pmatrix} & \\ \times \sqrt{(2n_1 + 1)(2n'_1 + 1)} \begin{pmatrix} n_1 & \lambda_1 & n'_1 \\ 0 & 0 & 0 \end{pmatrix} \begin{pmatrix} n_1 & \lambda_1 & n'_1 \\ -m_{n_1} & m_{\lambda_1} & m'_{n_1} \end{pmatrix} & \\ \times \sqrt{(2n_2 + 1)(2n'_2 + 1)} \begin{pmatrix} n_2 & \lambda_2 & n'_2 \\ 0 & 0 & 0 \end{pmatrix} \begin{pmatrix} n_2 & \lambda_2 & n'_2 \\ -m_{n_2} & m_{\lambda_2} & m'_{n_2} \end{pmatrix} & \\ \times \sqrt{(2l + 1)(2l' + 1)} \begin{pmatrix} l & \lambda_1 + \lambda_2 & l' \\ 0 & 0 & 0 \end{pmatrix} \begin{pmatrix} l & \lambda_1 + \lambda_2 & l' \\ -m_l & -(m_{\lambda_1} + m_{\lambda_2}) & m'_l \end{pmatrix}. & \quad (44) \end{aligned}$$

This provides the elements of the coupling matrix in Eq. (36) at long-range. From the properties of the 3-j symbols in Eq. (44), we find the following selection rules (in addition to the triangle relation selection rule):

- (i) $-m_{n_1} + m_{\lambda_1} + m'_{n_1} = 0$,
- (ii) $-m_{n_2} + m_{\lambda_2} + m'_{n_2} = 0$,
- (iii) $-m_l - (m_{\lambda_1} + m_{\lambda_2}) + m'_l = 0$,

which imply $m_{n_1} + m_{n_2} + m_l = m'_{n_1} + m'_{n_2} + m'_l$ or $M_J = M'_J$. There are no couplings if $M'_J \neq M_J$ showing that M_J is conserved during the collision.

4.4 Propagation. Log-derivative \mathbf{Z} matrix

To get all the radial functions $f(r)$, we need to solve the system of coupled equations Eq. (35). In reality, for practical and numerical reasons, the log-derivative of the radial functions is computed, rather than the functions themselves. This avoids numerical instabilities of the radial functions when a classically forbidden region is reached, and it avoids the necessity to compute the normalization of the functions at each r . We define the **log-derivative matrix** of the matrix $\mathbf{F}(r)$ in Eq. (39) by:

$$\mathbf{Z}(r) = \mathbf{F}' \mathbf{F}^{-1} = \left[\frac{d}{dr} \mathbf{F}(r) \right] \left[\mathbf{F}(r) \right]^{-1}. \quad (45)$$

The log-derivative matrix is a real and symmetric matrix so that $\mathbf{Z}^* = \mathbf{Z}$ and $\mathbf{Z}^t = \mathbf{Z}$. When $r \rightarrow r_{min} \simeq 0$, the potential energy surface becomes very repulsive due to the impenetrability of the particles. Then the radial functions become zero with no couplings, so that \mathbf{F} and \mathbf{Z} are diagonal. We then impose the initial log-derivative at $r = r_{min}$ to be:

$$\mathbf{Z}(r_{min}) = \infty \times \mathbf{I}. \quad (46)$$

If we divide the range of the radial coordinate r from r_{min} to r_{max} into small segments of width Δr (called sectors), one can propagate the log-derivative from sectors to sectors. Knowing what the log-derivative is in the previous sector, one can know what it is in the current sector. Because we know the log-derivative at $r_{min} \simeq 0$ we can propagate it to $r_{max} \simeq \infty$. We solve this way the system of coupled equations Eq. (35) for each r , called a close-coupling calculation. There are several efficient numerical methods to solve this set of equations, for example Refs. [74, 75, 76], which present no specific problems and can be routinely implemented. Those methods can compute not only the scattering properties of the coupled system with positive collision energies above the energy threshold of two initial separated particles, but also the presence of bound states with negative energies below the same threshold [78].

4.5 Symmetry considerations

We discuss in this section the role of the inversion and permutation symmetries and how they are handled in the quantum formalism. Inversion symmetry is considered when the potential energy does not include potentials that depend on the absolute position of the particles, while permutation symmetry is required when dealing

with collisions of identical particles. Including those symmetries will reduce the number of equations that are coupled in Eq. (35). Finally, we briefly discuss how the quantum formalism is modified when dealing with external potentials when for example electric or magnetic fields are applied.

Inversion symmetry

We consider here a potential energy V_{int} that do not depend on the absolute position of the particles, such as a potential energy surface of a system. The basis function in Eq. (29) turns out to be also an eigenfunction of the inversion parity operator \hat{I} . This operator corresponds to the transformation $(\vec{\rho}_1, \vec{\rho}_2, \vec{r}) \rightarrow (-\vec{\rho}_1, -\vec{\rho}_2, -\vec{r})$. This gives $\hat{I}\Phi_{\alpha l m_l}(\vec{\rho}_1, \vec{\rho}_2, \hat{r}) = \epsilon_I \Phi_{\alpha l m_l}(\vec{\rho}_1, \vec{\rho}_2, \hat{r})$ with the inversion parity quantum number $\epsilon_I \equiv (-1)^{n_1+n_2+l} = \pm 1$. This comes from the fact that the inversion symmetry of a vector $\vec{x} \rightarrow -\vec{x}$ is equivalent to $(x, \theta_x, \varphi_x) \rightarrow (x, \pi - \theta_x, \varphi_x + \pi)$ and thus implies $Y_j^{m_j}(-\hat{x}) = (-1)^j Y_j^{m_j}(\hat{x})$, while the radial wavefunction remains unchanged. If so, applying the inversion operator to a function depending on the radial coordinate like the coupling elements $\mathcal{U}^{int}(r)$ in Eq. (36) will let the function unchanged, $\hat{I}\mathcal{U}^{int}(r) = \mathcal{U}^{int}(r)$. On the other hand:

$$\begin{aligned} \hat{I}\mathcal{U}^{int}(r) &= \int d\vec{\rho}_1 d\vec{\rho}_2 d\hat{r} \Phi_{\alpha' l' m'_l}^*(-\vec{\rho}_1, -\vec{\rho}_2, -\hat{r}) U_{int}(-\vec{\rho}_1, -\vec{\rho}_2, -\vec{r}) \Phi_{\alpha l m_l}(\vec{\rho}_1, \vec{\rho}_2, \hat{r}) \\ &= \epsilon_I \epsilon'_I \int d\vec{\rho}_1 d\vec{\rho}_2 d\hat{r} \Phi_{\alpha' l' m'_l}^*(\vec{\rho}_1, \vec{\rho}_2, \hat{r}) U_{int}(-\vec{\rho}_1, -\vec{\rho}_2, -\vec{r}) \Phi_{\alpha l m_l}(\vec{\rho}_1, \vec{\rho}_2, \hat{r}). \end{aligned} \quad (47)$$

As the potential energy surface satisfies $U_{int}(-\vec{\rho}_1, -\vec{\rho}_2, -\vec{r}) = U_{int}(\vec{\rho}_1, \vec{\rho}_2, \vec{r})$, then $\epsilon_I \epsilon'_I = 1$ or $\epsilon_I = \epsilon'_I$. Inversion parity is then conserved in a collision involving a potential energy surface. This can be checked directly in Eq. (44). From the property of the 3-j symbols which contains the zero elements, these three symbols are non-zero if $(-1)^{n_1+\lambda_1+n'_1} = 1$, $(-1)^{n_2+\lambda_2+n'_2} = 1$, and $(-1)^{l+\lambda_1+\lambda_2+l'} = 1$. By arranging the $(-1)^{\lambda_1+\lambda_2}$ term, this implies $(-1)^{n_1+n_2+l} = (-1)^{n'_1+n'_2+l'}$ and then $\epsilon_I = \epsilon'_I$. This applies to collision of either identical or different molecules. Note that inversion is not always conserved in a collision if external potentials V_{ext} are included.

Permutation symmetry

If the two particles are identical, one also has to symmetrize the internal wavefunction $\phi_\alpha(\vec{\rho}_1, \vec{\rho}_2) = \phi_{\alpha_1}(\vec{\rho}_1) \phi_{\alpha_2}(\vec{\rho}_2)$ with respect to the permutation of the two particles operator \hat{P} . The permutation of the two particles is equivalent to the transformation $(\vec{\rho}_1, \vec{\rho}_2, \vec{r}) \rightarrow (\vec{\rho}_2, \vec{\rho}_1, -\vec{r})$. The properly symmetrized internal wavefunction is given by:

$$\phi_{\alpha\eta}(\vec{\rho}_1, \vec{\rho}_2) = \frac{1}{\sqrt{2(1 + \delta_{\alpha_1, \alpha_2})}} \left\{ \phi_{\alpha_1}(\vec{\rho}_1) \phi_{\alpha_2}(\vec{\rho}_2) + \eta \phi_{\alpha_2}(\vec{\rho}_1) \phi_{\alpha_1}(\vec{\rho}_2) \right\}. \quad (48)$$

$\eta = \pm 1$ describes, respectively, a symmetric and anti-symmetric internal wavefunction with respect to the permutation, so that $\hat{P}\phi_{\alpha\eta} = \eta\phi_{\alpha,\eta}$. Now the basis set functions in Eq. (29) become:

$$\Phi_{\alpha l m_l \eta}(\vec{\rho}_1, \vec{\rho}_2, \hat{r}) \equiv \phi_{\alpha\eta}(\vec{\rho}_1, \vec{\rho}_2) Y_l^{m_l}(\hat{r}), \quad (49)$$

and $\widehat{P}\Phi_{\alpha l m_l \eta} = \eta(-1)^l \Phi_{\alpha l m_l \eta}$ since $\vec{r} \rightarrow -\vec{r}$ is equivalent to $(r, \theta_r, \varphi_r) \rightarrow (r, \pi - \theta_r, \varphi_r + \pi)$ and $Y_l^{m_l}(-\hat{r}) = (-1)^l Y_l^{m_l}(\hat{r})$. One can show, using the above properly symmetrized basis set, that the coupled equations are diagonal in η .

Additionally, under permutation \widehat{P} of two identical particles, the total wavefunction has to obey the symmetrization principle:

$$\widehat{P}\psi^{E_{tot}} = \epsilon_P \psi^{E_{tot}} \quad (50)$$

with $\epsilon_P = +1$ if the (composite) particles are identical bosons and $\epsilon_P = -1$ if the (composite) particles are identical fermions. On the basis set functions, it gives $\widehat{P}\Phi = \epsilon_P \Phi$. Then this implies specific selection rules for η and l following the fact that $\eta(-1)^l = \epsilon_P$. In the case of identical bosons $\epsilon_P = +1$, internal wavefunctions of $\eta = +1$ (resp. $\eta = -1$) symmetry imply even partial waves $l = 0, 2, 4, \dots$ (resp. odd partial waves $l = 1, 3, 5, \dots$). In the case of identical fermions $\epsilon_P = -1$, internal wavefunctions of $\eta = +1$ (resp. $\eta = -1$) symmetry imply odd partial waves $l = 1, 3, 5, \dots$ (resp. even partial waves $l = 0, 2, 4, \dots$). Note that all values of l are included in the dynamics since both symmetries of η are generally allowed.

In the special case of indistinguishable particles, meaning particles in the same quantum state so that $\alpha_1 = \alpha_2$, Eq. (48) implies that the wavefunction for the $\eta = -1$ symmetry does not exist. In this special case, the number of partial waves describing the dynamics is reduced following the rules just mentioned above since only the $\eta = +1$ symmetry survives. This implies even partial waves $l = 0, 2, 4, \dots$ for indistinguishable bosons and odd partial waves $l = 1, 3, 5, \dots$ for indistinguishable fermions. At ultralow energy $E_c \rightarrow 0$, only the first and lowest partial wave is important for the dynamics. It is usually common to say that identical bosons in indistinguishable states collide in the s -wave (to refer to $l = 0$) and identical fermions in indistinguishable states collide in the p -wave (to refer to $l = 1$).

Collisions in external fields

Often in ultracold physics, additional external fields, such as electric or magnetic fields, are present to control the properties of the individual particles [28, 29] and their interactions [30]. Then, additional external potentials V_{ext} appear in the Hamiltonian of the system. The previous formalism remains unchanged except that the individual particles $i = 1, 2$ are now perturbed by the external field. As a consequence, the (bare) internal state of the particle ϕ_{α_i} in the absence of an external field is replaced with the corresponding (dressed) internal state $\tilde{\phi}_{\alpha_i}$ in the presence of the field. The dressed states are a linear combination of the bare states with given coefficients due to the interaction of the particle with the field. In the collision formalism, we just replace the individual bare states ϕ_{α_i} of the particles $i = 1, 2$ with their dressed states $\tilde{\phi}_{\alpha_i}$. To compute the elements of the coupling matrix in Eq. (36) between the dressed states $\tilde{\Phi}_{\alpha l m_l} = \tilde{\phi}_{\alpha_1} \tilde{\phi}_{\alpha_2} Y_l^{m_l}$, there is now just an additional step. We replace the dressed states by the expression of their linear combination of bare states and we compute the corresponding sum of all the bare elements. This presents no difficulties and is routinely done numerically. The other consequence is that J is not a good quantum number anymore, as mentioned

above, and an uncoupled representation basis set is generally preferred. The last section of this paper will illustrate such an example, where ultracold collisions of electric dipolar molecules of KRb occur in an external electric field.

5 Matching the two regions

To relate the observables far from the collision region to the potential energy and radial functions in the collision region, we will equate Eq. (14) and Eq. (27).

5.1 Reactance matrix \mathbf{K} . Relation with \mathbf{Z}

For practical and numerical reasons, the matching is not done at $r_{max} \simeq \infty$ but rather at r_{max} for which $|\mathcal{U}^{int}| \ll |\mathcal{U}^{cent}|$. This the distance for which the interaction terms (diagonal and non-diagonal) can be safely neglected compared to the centrifugal ones. The set of coupled equations Eq. (39) becomes diagonal, each diagonal elements taking the form:

$$\left\{ -\frac{\hbar^2}{2m_{red}} \frac{d^2}{dr^2} + \frac{\hbar^2 l(l+1)}{2m_{red}r^2} + \varepsilon - E_{tot} \right\} f(r) = 0, \quad (51)$$

each equations only differing by the values ε of the thresholds. This can also be written:

$$r^2 f''(r) + [k^2 r^2 - l(l+1)] f(r) = 0 \quad (52)$$

with the wavevector $k = \sqrt{2m_{red}(E_{tot} - \varepsilon)/\hbar^2}$. Two independent solutions are given by \tilde{j} and \tilde{n} , the Ricatti-Bessel functions and Ricatti-Neumann functions [79]. They are related to the spherical Bessel and spherical Neumann functions by $\tilde{j}_l = kr j_l(kr)$ and $\tilde{n}_l = kr n_l(kr)$ and to the Bessel and Neumann functions by $j_l(kr) = \sqrt{\pi/2kr} J_{l+1/2}(kr)$ and $n_l(kr) = \sqrt{\pi/2kr} N_{l+1/2}(kr)$. If we set $\rho = kr$, the solutions for the first l 's are:

$$\tilde{j}_0(\rho) = \sin(\rho) \quad \tilde{j}_1 = \frac{\sin(\rho)}{\rho} - \cos(\rho) \quad (53)$$

$$\tilde{n}_0(\rho) = -\cos(\rho) \quad \tilde{n}_1 = -\frac{\cos(\rho)}{\rho} - \sin(\rho). \quad (54)$$

The behaviour for $\rho \rightarrow 0$ is:

$$\tilde{j}_l(\rho) \underset{\rho \rightarrow 0}{\propto} \frac{\rho^{l+1}}{(2l+1)!!} \quad \tilde{n}_l(\rho) \underset{\rho \rightarrow 0}{\propto} -(2l-1)!! \rho^{-l} \quad (55)$$

with $x!! = x(x-2)(x-4)\dots$ \tilde{j} are often called regular functions since $\tilde{j} \rightarrow 0$ as $\rho \rightarrow 0$ and \tilde{n} are often called irregular functions since $\tilde{n} \rightarrow \pm\infty$ as $\rho \rightarrow 0$. For $\rho \rightarrow \infty$:

$$\tilde{j}_l(\rho) \underset{\rho \rightarrow \infty}{\propto} \sin(\rho - l\pi/2) \quad \tilde{n}_l(\rho) \underset{\rho \rightarrow \infty}{\propto} -\cos(\rho - l\pi/2). \quad (56)$$

A general solution of Eq. (51) for the radial functions at $r = r_{max}$ is given by:

$$\mathbf{F}(r) = \mathbf{F}^{(1)} \mathbf{A} + \mathbf{F}^{(2)} \mathbf{B} \Big|_{r=r_{max}} \quad (57)$$

where:

$$F_{i',i}^{(1)} = \delta_{i',i} \frac{1}{k_{\alpha'}^{1/2}} \tilde{j}_{i'}(k_{\alpha'} r) \quad F_{i',i}^{(2)} = \delta_{i',i} \frac{1}{k_{\alpha'}^{1/2}} \tilde{n}_{i'}(k_{\alpha'} r). \quad (58)$$

\mathbf{A}, \mathbf{B} are real constant matrices, independent of r . In the special case without coupling terms, that is no off-diagonal terms in Eq. (39) $\forall r$, the system is uncoupled and \mathbf{A}, \mathbf{B} will be diagonal at $r = r_{max}$. More generally when coupling terms are present for $r < r_{max}$ in Eq. (39), the system is coupled and \mathbf{A}, \mathbf{B} will be full matrices in general at $r = r_{max}$. We can also write Eq. (57) as:

$$\mathbf{F}(r) = \mathbf{F}^K(r) \mathbf{N}^K \Big|_{r=r_{max}} \quad (59)$$

with:

$$\mathbf{F}^K(r) = \{\mathbf{F}^{(1)} - \mathbf{F}^{(2)} \mathbf{K}\}. \quad (60)$$

\mathbf{K} is called the **reactance matrix**. \mathbf{N}^K is a real normalisation matrix. From Eq. (57), Eq. (59) and Eq. (60), $\mathbf{K} \equiv -\mathbf{B} \mathbf{A}^{-1}$ and $\mathbf{N}^K \equiv \mathbf{A}$. The superscript K indicates that the radial functions obey boundary conditions of the \mathbf{K} matrix. The \mathbf{K} matrix is real as the matrices \mathbf{A}, \mathbf{B} are real. The off-diagonal matrix elements of \mathbf{K} provide an indication of the character of the other final channels due to the couplings from the interaction potential energy of the system in the wavefunction, for a given incident initial colliding channel. We chose the factors $k_{\alpha'}^{-1/2}$ in the two linearly independent functions $\mathbf{F}^{(1)}, \mathbf{F}^{(2)}$ so that the **Wronskian matrix** $\mathbf{W} = \mathbf{F}^{(1)} \mathbf{F}'^{(2)} - \mathbf{F}'^{(1)} \mathbf{F}^{(2)}$ is the identity matrix \mathbf{I} . If so, \mathbf{K} is also a symmetric matrix. This is shown in Proof 1 of the appendix of this paper. \mathbf{K} is related to the \mathbf{Z} matrix by (the order of the matrix multiplication is important to get a symmetric matrix):

$$\mathbf{K} = \left\{ \mathbf{Z} \mathbf{F}^{(2)} - \mathbf{F}'^{(2)} \right\}^{-1} \left\{ \mathbf{Z} \mathbf{F}^{(1)} - \mathbf{F}'^{(1)} \right\} \Big|_{r=r_{max}}. \quad (61)$$

This is often referred to as the matching procedure, performed at $r = r_{max}$. This is shown in Proof 2 of the appendix. From the proof, one can see that the reactance matrix is independent of the choice of the normalisation matrix \mathbf{N}^K of the radial functions. It depends only on its log-derivative matrix \mathbf{Z} at r_{max} : if \mathbf{Z} is diagonal (non-diagonal) due to the uncoupled (coupled) Schrödinger equations, \mathbf{K} is diagonal (non-diagonal).

5.2 Scattering matrix S. Relation with K

The problem with Eq. (59) is that the functions are not written in terms of incoming and outgoing radial functions, as the ones appearing in the asymptotic wavefunction in Eq. (14). When $r \rightarrow \infty$ in Eq. (59), Eq. (56) shows that the Ricatti-Bessel and Ricatti-Neumann functions behave as sine and cosine functions which can also be written in terms of incoming/outgoing spherical wave. Another general solution of Eq. (51) for the radial functions is then given by:

$$\mathbf{F}(r) \underset{r \rightarrow \infty}{=} \mathbf{F}^{(-)} \mathbf{A}' + \mathbf{F}^{(+)} \mathbf{B}', \quad (62)$$

where

$$F_{i',i}^{\pm} = \delta_{i',i} \frac{1}{k_{\alpha'}^{1/2}} e^{\pm i(k_{\alpha'} r - l' \pi/2)} \quad (63)$$

are incoming (-) or outgoing (+) spherical waves and \mathbf{A}' , \mathbf{B}' are complex constant matrices, independent of r . Again, in the special case without coupling terms $\forall r$ in Eq. (39), \mathbf{A}' and \mathbf{B}' will be diagonal while they will be full matrices if coupling terms are present. We can also write Eq. (62) as:

$$\mathbf{F}(r) \underset{r \rightarrow \infty}{=} \mathbf{F}^S(r) \mathbf{N}^S \quad (64)$$

with:

$$\mathbf{F}^S(r) = \{\mathbf{F}^- - \mathbf{F}^+ \mathbf{S}\}. \quad (65)$$

\mathbf{S} is the **scattering matrix**. \mathbf{N}^S is a complex normalisation matrix. The superscript S indicates now that the radial functions obey boundary conditions of the \mathbf{S} matrix. Eq. (64) is the useful form to match with the asymptotic one in Eq. (14) because it uses incoming and outgoing radial functions as well. From Eq. (62), Eq. (64) and Eq. (65), $\mathbf{S} \equiv -\mathbf{B}' \mathbf{A}'^{-1}$ and $\mathbf{N}^S \equiv \mathbf{A}'$. \mathbf{S} is related to the \mathbf{K} matrix by:

$$\mathbf{S} = \frac{\mathbf{I} + i\mathbf{K}}{\mathbf{I} - i\mathbf{K}}. \quad (66)$$

This is shown in Proof 3 of the appendix. Again from the proof, one can see that the scattering matrix is independent of the normalization matrix \mathbf{N}^S of the radial functions. It depends only on the reactance matrix, and hence the log-derivative matrix. \mathbf{S} is a symmetric matrix: $\mathbf{S}^t = \mathbf{S}$, and a unitary matrix: $\mathbf{S} \mathbf{S}^\dagger = \mathbf{S}^\dagger \mathbf{S} = \mathbf{I}$, as shown in Proof 4 of the appendix. \mathbf{S} in general is a complex matrix including a real and imaginary part. The coefficient of the outgoing waves in the channel i' coming from an incoming wave in the channel i is given by the element $S_{i',i}$. The elements $|S_{i',i}|^2$ correspond to the ratio of the outgoing flux $4\pi\hbar|S_{i',i}|^2/m_{red}$ over the incoming one $4\pi\hbar/m_{red}$ in absolute value (one can compute the flux using Eq. (5) and Eq. (3), using the radial functions in Eq. (63) and integrating over the whole solid angle $d\hat{r}$). Then the probability to collide from a state i to a state i' is simply given by

$$P_{i \rightarrow i'} = |S_{i',i}|^2 \quad \text{with:} \quad \sum_{i'} P_{i \rightarrow i'} = 1. \quad (67)$$

Finally, we impose a diagonal normalization matrix \mathbf{N}^S in Eq. (64). This enables that an independent solution of the Schrödinger equation, corresponding to a given column of the \mathbf{F} matrix given by Eq. (64), has the same overall normalization in a multiplicative factor, as suggested by Eq. (27). In that way, the diagonal elements of this matrix identify directly with the normalization factor we have already defined in Eq. (27) so that $N_{\alpha l m_l, \alpha l m_l}^S \equiv N_{\alpha l m_l}$.

5.3 Transition matrix \mathbf{T} . Relation with observables

At $r_{max} \simeq \infty$, $\mathcal{U}^{int}, \mathcal{U}^{cent} \rightarrow 0$ in Eq. (34), the wavefunction tends to Eq. (14) far from the collision region:

$$\psi_{\alpha, \vec{k}_\alpha}^{E_{tot}} \underset{r \rightarrow \infty}{=} \mathcal{A} \left[e^{i\vec{k}_\alpha \cdot \vec{r}} \phi_\alpha + \sum_{\alpha'} f_{\alpha \rightarrow \alpha'}^+ \frac{e^{ik_{\alpha'} r}}{r} \phi_{\alpha'} \right] = \psi_{inc} + \psi_{scat}, \quad (68)$$

where ψ_{inc} has the form of Eq. (23). When no interaction potential energy is present, no scattering is present ($\psi_{scat} = 0$), we see that $\psi_{\alpha, \vec{k}_\alpha} = \psi_{inc}$ contains only the initial internal state ϕ_α and for which the radial function is a superposition of an incoming and outgoing spherical wave $e^{\pm i(k_\alpha r - l\pi/2)}/r$, of same amplitudes. In the presence of the interaction potential energy term U_{int} , the scattering wave ψ_{scat} will additionally produce outgoing spherical waves $e^{i(k_{\alpha'} r - l'\pi/2)}/r$ in final states $\phi_{\alpha'}$, responsible for inelastic transitions. Both the asymptotic expansion Eq. (14) and the partial wave expansion Eq. (27) and Eq. (28), using Eq. (64), contain now an incoming and outgoing spherical wave term. One can then identify their expressions. This leads to the expression of the normalization factor of each partial waves in Eq. (27):

$$N_{\alpha l m_l}(\vec{k}_\alpha) = \mathcal{A} \frac{2\pi i}{k_\alpha^{1/2}} i^l [Y_l^{m_l}(\hat{k}_\alpha)]^*. \quad (69)$$

Similarly, the scattering amplitude in Eq. (14) writes:

$$f_{\alpha \rightarrow \alpha'}^+(\vec{k}_\alpha, \hat{r}) = \frac{2\pi}{i k_\alpha^{1/2} k_{\alpha'}^{1/2}} \sum_{l=0}^{\infty} \sum_{m_l=-l}^l \sum_{l'=0}^{\infty} \sum_{m'_l=-l'}^{l'} i^{l-l'} [Y_l^{m_l}(\hat{k}_\alpha)]^* Y_{l'}^{m'_l}(\hat{r}) T_{\alpha' l' m'_l, \alpha l m_l}(k_\alpha) \quad (70)$$

in terms of the **transition matrix**:

$$\mathbf{T} = \mathbf{S} - \mathbf{I}. \quad (71)$$

Note that some references use a definition $\mathbf{T} = \mathbf{I} - \mathbf{S}$ but the scattering amplitude is then defined with a factor of $2\pi i$ instead of $2\pi/i$ in Eq. (70), which provides in any case the same scattering amplitude. One can then get the observables in terms of the \mathbf{T} matrix. The differential cross section is given by Eq. (16):

$$\begin{aligned} \frac{\partial \sigma_{\alpha \rightarrow \alpha'}(\vec{k}_\alpha, \hat{r})}{\partial \hat{r} \partial \vec{k}_\alpha} &= \frac{k_{\alpha'}}{k_\alpha} |f_{\alpha \rightarrow \alpha'}^+(\vec{k}_\alpha, \hat{r})|^2 \\ &= \frac{4\pi^2}{k_\alpha^2} \sum_{l_a} \sum_{m_{l_a}} \sum_{l_b} \sum_{m_{l_b}} \sum_{l_c} \sum_{m_{l_c}} \sum_{l_d} \sum_{m_{l_d}} i^{-l_a+l_b+l_c-l_d} \\ &\quad \times Y_{l_a}^{m_{l_a}}(\hat{k}_\alpha) [Y_{l_b}^{m_{l_b}}(\hat{r})]^* [Y_{l_c}^{m_{l_c}}(\hat{k}_\alpha)]^* Y_{l_d}^{m_{l_d}}(\hat{r}) \\ &\quad \times T_{\alpha' l_a m_{l_a}, \alpha l_b m_{l_b}}^*(k_\alpha) T_{\alpha' l_c m_{l_c}, \alpha l_d m_{l_d}}(k_\alpha), \quad (72) \end{aligned}$$

where running indexes $l_a, m_{l_a}, \dots, l_d, m_{l_d}$ have been used in the expression of the modulus squared of the scattering amplitude. The averaged integral cross section is given by Eq. (18):

$$\begin{aligned}\sigma_{\alpha \rightarrow \alpha'}(E_c) &= \Delta \times \frac{\pi}{k_\alpha^2} \sum_l \sum_{m_l} \sum_{l'} \sum_{m'_l} |T_{\alpha' l' m'_l, \alpha l m_l}(k_\alpha)|^2 \\ &= \sum_l \sum_{m_l} \sigma_{\alpha \rightarrow \alpha', l m_l}(E_c),\end{aligned}\tag{73}$$

where we can define a partial wave cross section $\sigma_{\alpha \rightarrow \alpha', l m_l}$. From Eq. (72) to Eq. (73), we used the fact that the integration over \hat{k}_α gives $\delta_{l_a, l_c} \delta_{m_{l_a}, m_{l_c}}$ and the integration over \hat{r} gives $\delta_{l_b, l_d} \delta_{m_{l_b}, m_{l_d}}$. In the case of identical particles starting in indistinguishable states ($\phi_\alpha = \phi_{\alpha_1} \phi_{\alpha_2}$ with $\alpha_1 = \alpha_2$), one has to multiply the cross sections by a factor $\Delta = 2$ for symmetry reasons as the differential cross sections have to be integrated over half space only [80, 81]. Note that in this case the number of partial waves is halved compared to the case of identical but distinguishable or different particles, due to the specific rules mentioned above for the partial waves. In the case of identical particles starting in distinguishable states ($\alpha_1 \neq \alpha_2$), or in the case of different particles, $\Delta = 1$. Eq. (20) is used to obtain the corresponding rate coefficient. In a numerical calculation, one usually computes the $\mathbf{Z}, \mathbf{K}, \mathbf{S}, \mathbf{T}$ matrices in this order to get the observables.

5.4 Link to scattering of structureless particles. The central potential problem

It is interesting to see how to recover the central potential problem for elastic scattering of structureless particles (that can be found in many textbooks [47, 48, 49, 50, 51, 52]), from the more general elastic and inelastic scattering formalism of particles with internal structure presented in this paper. First, in the central potential problem the interaction is assumed to be isotropic, $U_{int}(\vec{r}) = U_{int}(r)$, so that it does not depend on the angles \hat{r} . Then the operators $\widehat{H}, \widehat{L}^2, \widehat{L}_z$ commute and l, m_l are good quantum numbers which are conserved during the collision, in addition with the total energy. So $l' = l$ and $m'_l = m_l$. Secondly, for an elastic collision, $\alpha' = \alpha$. Finally, the collision does not depend on the direction of the incident particles since the potential is isotropic. One can choose for example the direction $\hat{k}_\alpha \equiv \hat{z} = (0, 0)$. Then $[Y_l^{m_l}(0, 0)]^* \equiv \sqrt{2l+1/4\pi} \delta_{m_l, 0}$, this implies $m_l = 0$. The asymptotic expansion writes:

$$\psi_k^{E_{tot}} \underset{r \rightarrow \infty}{=} A \left[e^{ikz} + f^+(k, \hat{r}) \frac{e^{ikr}}{r} \right].\tag{74}$$

Then the scattering amplitude reduces to:

$$\begin{aligned}
f_{\alpha \rightarrow \alpha}^+(\vec{k}_\alpha, \hat{r}) &= f^+(k_\alpha, \hat{r}) \\
&= \frac{2\pi}{i k_\alpha^{1/2} k_{\alpha'}^{1/2}} \sum_{l=0}^{\infty} \sum_{m_l=-l}^l \sum_{l'=0}^{\infty} \sum_{m'_l=-l'}^{l'} i^{l-l'} [Y_l^{m_l}(\hat{k}_\alpha)]^* Y_{l'}^{m'_l}(\hat{r}) T_{\alpha' l' m'_l, \alpha l m_l}(k_\alpha) \\
&= \frac{2\pi}{i k_\alpha} \sum_{l=0}^{\infty} i^0 \sqrt{\frac{2l+1}{4\pi}} \delta_{m_l, 0} Y_l^0(\hat{r}) T_{\alpha l 0, \alpha l 0}(k_\alpha) \\
&= \frac{2\pi}{i k} \sum_{l=0}^{\infty} i^0 \sqrt{\frac{2l+1}{4\pi}} \sqrt{\frac{2l+1}{4\pi}} P_l^0(\cos \theta) T_l \\
&= \frac{1}{2 i k} \sum_{l=0}^{\infty} (2l+1) P_l^0(\cos \theta) T_l
\end{aligned} \tag{75}$$

and the cross section reduces to:

$$\begin{aligned}
\sigma(k) &= \int d\hat{r} |f^+|^2 \\
&= \frac{1}{4k^2} \sum_{l=0}^{\infty} \sum_{l'=0}^{\infty} (2l+1) (2l'+1) \left[\int d\hat{r} P_l^0(\cos \theta) P_{l'}^0(\cos \theta) \right] T_l^* T_{l'} \\
&= \frac{\pi}{k^2} \sum_{l=0}^{\infty} (2l+1) |T_l|^2.
\end{aligned} \tag{76}$$

From Eq. (75) to Eq. (76), we used $\int_0^\pi P_l^0 P_{l'}^0 \sin \theta d\theta = 2/(2l+1) \delta_{l,l'}$ and $\int_0^{2\pi} d\varphi = 2\pi$. Because for elastic collisions, the \mathbf{S} matrix reduces to an element for a given l , it can be written $S_l = e^{2i\delta_l(k)}$. $\delta_l(k)$ is called the **scattering phase shift** in the partial wave l . Since there are no inelastic channels then $|S_l|^2 = 1$. The role of the central potential is then to shift the phase of the outgoing wave by $\delta_l(k)$. By noting that $1 - e^{2i\delta_l(k)} = e^{i\delta_l(k)}(e^{-i\delta_l(k)} - e^{i\delta_l(k)}) = -2i e^{i\delta_l(k)} \sin \delta_l(k)$, one can also find:

$$\sigma(k) = \frac{4\pi}{k^2} \sum_{l=0}^{\infty} (2l+1) \sin^2 \delta_l(k) \tag{77}$$

which is a formula often quoted in textbooks. The phase shift is related to the K matrix by $K_l = \tan \delta_l$. Note that we recover Eq. (66) because:

$$S_l = e^{2i\delta_l} = \frac{1 + i \tan \delta_l}{1 - i \tan \delta_l} = \frac{1 + iK_l}{1 - iK_l}. \tag{78}$$

We used the fact that $1 \pm i \tan \delta = 1 \pm \frac{e^{i\delta} - e^{-i\delta}}{e^{i\delta} + e^{-i\delta}} = \frac{2e^{\pm i\delta}}{e^{i\delta} + e^{-i\delta}}$.

6 Behaviour at ultralow energy. Scattering length and threshold laws

We now present how the dynamics of two colliding particles behaves at ultralow energy when $E_c \rightarrow 0$. To simplify the discussion, we will take the case of an elastic

collision of structureless particles interacting with a central potential $U_{int}(r)$, as described in the previous section. The Schrödinger equation writes:

$$\left\{ -\frac{\hbar^2}{2m_{red}} \frac{d^2}{dr^2} + \frac{\hbar^2 l(l+1)}{2m_{red}r^2} + \mathcal{U}^{int}(r) - E_c \right\} f(r) = 0 \quad (79)$$

where $E_c = \hbar^2 k^2 / 2m_{red}$ (we take the energy of the two separated particles as the reference energy). The matching procedure Eq. (61) is performed at $r_{max} = r_0$ where r_0 denotes the typical distance for which $|\mathcal{U}^{int}(r_0)| \ll |\mathcal{U}^{cent}(r_0)|$. On one hand, there is always a typical collision energy E_c^* for and below which $E_c \ll |\mathcal{U}^{int}(r_0)|, |\mathcal{U}^{cent}(r_0)|$ so that the Schrödinger equation is in this limit independent of E_c at r_0 . Then, the function and its derivative at $r = r_0$ are also independent of E_c . Its log-derivative is then a given constant $Z = C$ at $r = r_0$. On the other hand, from Eq. (60), we know the general form of $f(r) = f^{(1)}(\rho) - f^{(2)}(\rho) K_l = \tilde{j}(\rho)/\sqrt{k} - \tilde{n}(\rho)/\sqrt{k} K_l$ (using $\rho = kr$) and its derivative $f'(r) = f'^{(1)}(kr) - f'^{(2)}(kr) K_l$, the prime being a derivative with respect to r . If we use $d/dr = k d/d\rho$, we have $f'(r) = k(df^{(1)}(\rho)/d\rho) - k(df^{(2)}(\rho)/d\rho) K_l = \sqrt{k}(d\tilde{j}(\rho)/d\rho) - \sqrt{k}(d\tilde{n}(\rho)/d\rho) K_l$. We perform the matching procedure at $r_{max} = r_0$, using Eq. (55) for the functions and their derivatives as $E_c, k \rightarrow 0$, using a constant energy-independent value of the log-derivative $Z = C$, and using the fact that $K_l = \tan(\delta_l)$ where δ_l is the scattering phase shift (see the central potential problem above). Eq. (61) gives [47]:

$$\begin{aligned} \tan(\delta_l) &= \frac{Z_l f^{(1)} - f'^{(1)}}{Z_l f^{(2)} - f'^{(2)}} \\ &= \frac{C \tilde{j}(\rho)/\sqrt{k} - \sqrt{k}(d\tilde{j}(\rho)/d\rho)}{C \tilde{n}(\rho)/\sqrt{k} - \sqrt{k}(d\tilde{n}(\rho)/d\rho)} \\ &= \frac{C \tilde{j}(\rho) - k(d\tilde{j}(\rho)/d\rho)}{C \tilde{n}(\rho) - k(d\tilde{n}(\rho)/d\rho)} \\ &\stackrel{\rho \rightarrow 0}{=} -\frac{1}{(2l+1)!!(2l-1)!!} \frac{C D \rho^{l+1} - E k \rho^l}{C F \rho^{-l} - G k \rho^{-l-1}} \\ &\stackrel{k \rightarrow 0}{=} -\frac{(2l+1)}{[(2l+1)!!]^2} \frac{C D k^{l+1} r_0^{l+1} - E k^{l+1} r_0^l}{C F k^{-l} r_0^{-l} - G k^{-l} r_0^{-l-1}} \\ &\stackrel{k \rightarrow 0}{=} -\frac{(2l+1)}{[(2l+1)!!]^2} \left(\frac{C D r_0^{l+1} - E r_0^l}{C F r_0^{-l} - G r_0^{-l-1}} \right) k^{2l+1} \\ &\stackrel{k \rightarrow 0}{=} -\mathcal{L} k^{2l+1} \end{aligned} \quad (80)$$

where D, E, F, G are dimensionless proportionality factors in Eq. (55). Since C and k have the dimension of an inverse length and $\tan(\delta_l)$ has no units, the constant \mathcal{L} has the dimension of a length to the power $2l+1$. The most important partial wave to describe the collision at ultralow energies corresponds to the first lowest partial wave. For identical and indistinguishable bosonic particles or for different particles, the first partial wave is $l = 0$ as mentioned earlier, then \mathcal{L} has the dimension of a length. We define the **s-wave scattering length** by:

$$a_s = \lim_{k \rightarrow 0} -\frac{\tan \delta_{l=0}(k)}{k}. \quad (81)$$

The cross section can be linked to the scattering length by:

$$\begin{aligned}
\sigma_{l=0}(k) &= \frac{4\pi}{k^2} \sin^2 \delta_0(k) = \frac{4\pi}{k^2} \frac{1}{\frac{\sin^2 \delta_0(k) + \cos^2 \delta_0(k)}{\sin^2 \delta_0(k)}} \\
&= \frac{4\pi}{k^2} \frac{1}{1 + \frac{1}{\tan^2 \delta_0(k)}} = \frac{4\pi}{k^2} \frac{1}{1 + \frac{1}{(a_s k)^2}} \\
&\xrightarrow{k \rightarrow 0} 4\pi a_s^2. \tag{82}
\end{aligned}$$

This cross section is the same than the one provided by a hard sphere potential of radius a_s , that is $U^{int}(r) = \infty$ if $r \leq a_s$, 0 otherwise. Then at ultralow energy, one can safely replace a complicated interaction potential energy by a simple hard sphere model potential, since the cross sections will be the same. The model potential represents a simple, effective potential for the collision of the system, for which the scattering length plays the essential parameter. In ultracold physics in many-body interacting systems, the scattering length plays a crucial role in terms of which the many-body physics is described. It appears, for example, in the Gross–Pitaevskii equations to describe the physics of ultracold gases of particles in interaction [82, 83]. For identical and indistinguishable fermionic particles, the first partial wave is $l = 1$, then \mathcal{L} is a volume. We define the **p-wave scattering length** (the volume \mathcal{L} is the cube of this length) by:

$$a_p^3 = \lim_{k \rightarrow 0} - \frac{\tan \delta_{l=1}(k)}{k^3}. \tag{83}$$

The result in Eq. (80), Eq. (81) and Eq. (83) are not generally valid for potentials falling off asymptotically as an inverse power of the distance r . Also, for interaction potential $U^{int}(r) = \pm C_s/r^s$, with $s > 2$, the threshold behaviour in Eq. (80) is dominant for partial waves $l < (s - 3)/2$ [49, 51, 84, 85]. For partial waves $l > (s - 3)/2$, the dominant threshold behaviour becomes:

$$\tan(\delta_l) \underset{k \rightarrow 0}{\propto} k^{s-2}. \tag{84}$$

For partial waves $l = (s - 3)/2$, both contributions Eq. (80) and Eq. (84) are taken to describe the threshold behaviour. Using Eq. (77) and Eq. (82), the behaviour of the elastic cross sections and rate coefficients at a vanishing collision energy becomes when using the threshold behaviour Eq. (80):

$$\sigma_l^{el} \underset{k, E_c \rightarrow 0}{\propto} k^{4l} \propto E_c^{2l} \qquad \beta_l^{el} \underset{k, E_c \rightarrow 0}{\propto} k^{4l+1} \propto E_c^{2l+1/2}. \tag{85}$$

When using the threshold behaviour Eq. (84), it becomes:

$$\sigma_l^{el} \underset{k, E_c \rightarrow 0}{\propto} k^{2s-6} \propto E_c^{s-3} \qquad \beta_l^{el} \underset{k, E_c \rightarrow 0}{\propto} k^{2s-5} \propto E_c^{s-5/2}. \tag{86}$$

Inelastic/reactive cross sections and rate coefficients behaviours are given without proof [86]:

$$\sigma_l^{in/re} \underset{k, E_c \rightarrow 0}{\propto} k^{2l-1} \propto E_c^{l-1/2} \qquad \beta_l^{in/re} \underset{k, E_c \rightarrow 0}{\propto} k^{2l} \propto E_c^l. \tag{87}$$

These expressions are called the **threshold laws** or **Wigner laws** [86].

7 Application to ultracold collisions of dipolar molecules in electric fields

In 2008, a major breakthrough has been made in the field of ultracold molecular physics with the production of a dense and coherent gas of ultracold dipolar fermionic $^{40}\text{K}^{87}\text{Rb}$ molecules [24]. In contrast with the previous experiments of that time [30], these molecules were produced in their ground electronic state $^1\Sigma^+$, their ground vibrational state $v = 0$, and their ground rotational state $n = 0$, with additional control over the hyperfine states [87]. Therefore, the experimentalists were able to address the internal state of all the molecules of a dense gas to the absolute ground state. The molecule of KRb possesses in its own frame a permanent electric dipole moment of $d = 0.57$ D[24]. Therefore, the energy of the molecules and their interactions can be manipulated with an external electric field. KRb molecules are also chemically reactive even in their absolute ground state [88, 89, 90] so that $\text{KRb} + \text{KRb} \rightarrow \text{K}_2 + \text{Rb}_2$ is an exoergic process. On the one hand, this is a drawback for creating long-lived gases of strong dipolar ultracold molecules in experiments since this chemical reaction will lead to large molecular losses. But on the other hand if an electric field is applied, the molecular losses, which can be quite easily measured in a experiment as a function of time, will directly provide a signature of the dipolar interaction of the colliding molecules. It is therefore important to understand the collisional properties of the dipolar gas, in terms of its stability and lifetime. Collisions are also driving the thermal equilibrium of the gas and are very important to perform evaporative cooling to further decrease the temperature and reach eventually quantum degeneracy, as it was performed for ultracold gases of atoms [4, 5]. As an illustration of the formalism studied in this paper, we will present in this section the collisional properties of $\text{KRb} + \text{KRb} \rightarrow \text{K}_2 + \text{Rb}_2$ as a function of an electric field, for $^1\Sigma^+$, $v = 0$ molecules initially in the ground rotational state $n = 0$ and in the first excited rotational state $n = 1$, for both fermionic $^{40}\text{K}^{87}\text{Rb}$ molecules and bosonic $^{41}\text{K}^{87}\text{Rb}$ molecules. The spin structure of the molecules will not be taken into account in the following.

7.1 A simplified problem

The full time-independent quantum mechanical formalism developed previously still represents a numerical challenge for diatom-diatom or polyatomic molecular collisions at the present time:

(i) Firstly, full potential energy surfaces of polyatomic systems (involving all degrees of freedom) are generally challenging to compute, especially in the region of the complex where the atoms are close to each other. This is still feasible for tri-atomic systems but becomes in general difficult for tetra-atomic ones.

(ii) Secondly, when systems are chemically reactive, the Jacobi coordinates used in the present formalism are not appropriate anymore. Instead, one has to use hyperspherical coordinates [56, 57] as already mentioned, which treat, in a symmetric way, the polyatomic system formed by the atoms. The hyperspherical formalism [58, 59, 60] is well adapted for proper symmetrization of the overall wavefunction with respect to identical atom exchange as well as treating the products of a

chemical reaction. However, the formalism becomes difficult to handle numerically, especially using a full potential energy surface. Consequently, chemically reactive collision of diatomic molecules have to be tackled in another way at the present time. To overcome those problems, we will use two assumptions to treat the collisions of two diatomic reactive molecules.

Long-range interaction

First we will consider only the long-range interaction of the potential energy so that $U_{int} = U_{mult}$. At ultralow collision energies, the dynamics becomes more and more sensitive to the term that is the most longer-ranged in the potential energy. In the case of neutral diatomic molecules which possess an electric dipole moment, like KRb, the most longer-ranged term in the multipole-multipole interaction is the dipole-dipole interaction ($\lambda_1 = \lambda_2 = 1, \lambda = 2$ in Eq. (44)), so that $U_{mult} = U_{dd}$. The matrix elements in the uncoupled basis presented above for a diatomic molecule are given by:

$$\begin{aligned}
& \langle n_1, m_{n_1}, n_2, m_{n_2}, l, m_l | U_{dd} | n'_1, m'_{n_1}, n'_2, m'_{n_2}, l', m'_l \rangle = \\
& -\sqrt{30} \frac{d^2}{4\pi\epsilon_0 r^3} \sum_{m_{\lambda_1} m_{\lambda_2}} (-1)^{m_{n_1} + m_{n_2} + m_l} \begin{pmatrix} 1 & 1 & 2 \\ m_{\lambda_1} & m_{\lambda_2} & -(m_{\lambda_1} + m_{\lambda_2}) \end{pmatrix} \\
& \times \sqrt{(2n_1 + 1)(2n'_1 + 1)} \begin{pmatrix} n_1 & 1 & n'_1 \\ 0 & 0 & 0 \end{pmatrix} \begin{pmatrix} n_1 & 1 & n'_1 \\ -m_{n_1} & m_{\lambda_1} & m'_{n_1} \end{pmatrix} \\
& \times \sqrt{(2n_2 + 1)(2n'_2 + 1)} \begin{pmatrix} n_2 & 1 & n'_2 \\ 0 & 0 & 0 \end{pmatrix} \begin{pmatrix} n_2 & 1 & n'_2 \\ -m_{n_2} & m_{\lambda_2} & m'_{n_2} \end{pmatrix} \\
& \times \sqrt{(2l + 1)(2l' + 1)} \begin{pmatrix} l & 2 & l' \\ 0 & 0 & 0 \end{pmatrix} \begin{pmatrix} l & 2 & l' \\ -m_l & -(m_{\lambda_1} + m_{\lambda_2}) & m'_l \end{pmatrix} \quad (88)
\end{aligned}$$

where $d \equiv Q_{10}$ is the electric dipole moment. Higher multipole terms such as the quadrupole and octopole terms [91] can become important at higher collision energies [92]. In addition to the dipole-dipole term, we include a diagonal electronic $-C_6/r^6$ van der Waals interaction [93, 94, 95].

A short-range tunable condition

Secondly, we will use a phenomenological approach to treat the molecular collisions at short-range. The initial condition for the propagation of the radial wavefunction was given by a diagonal matrix in Eq. (46) corresponding to an infinite wall at $r = r_{min}$. We will now slightly modify this condition. We still keep the matrix diagonal, meaning no couplings between channels at short-range, but we now allow some additional effective scattering phase-shift and some effective loss for each channels due to the result of the (unknown) potential energy surface at short-range. We then construct a flexible and tunable log-derivative matrix, where the diagonal elements

for a channel i are given by [92]:

$$\begin{aligned} Z_{i,i}(r = r_{min}) &= \frac{4 k_{min} s c \sqrt{1 - p_{SR}}}{c^2 (\sqrt{1 - p_{SR}} - 1)^2 + s^2 (\sqrt{1 - p_{SR}} + 1)^2} \\ &- i \frac{k_{min} p_{SR}}{c^2 (\sqrt{1 - p_{SR}} - 1)^2 + s^2 (\sqrt{1 - p_{SR}} + 1)^2}, \end{aligned} \quad (89)$$

where:

$$k_{min} = \sqrt{\frac{2 m_{red} [E_{tot} - \mathcal{U}_{i,i}^{eff}(r = r_{min})]}{\hbar^2}} \quad (90)$$

and:

$$c = \cos(k_{min} r_{min} + \delta_{SR}) \quad s = \sin(k_{min} r_{min} + \delta_{SR}). \quad (91)$$

The log-derivative at r_{min} can be continuously tuned by two parameters $0 \leq p_{SR} \leq 1$ and $0 \leq \delta_{SR} \leq \pi$. p_{SR} represents a loss probability for the flux coming from the long-range region $r > r_{min}$ describing phenomenologically a loss at short-range, while δ_{SR} represents a phase shift accumulated from the short-range region $r < r_{min}$, describing phenomenologically the result of the (unknown) potential energy surface there. The above log-derivative condition has been constructed at $r = r_{min}$ so that it describes a square well of constant depth $\mathcal{U}_{i,i}^{eff}(r_{min})$ given by Eq. (38) from $r = 0$ to $r = r_{min}$, with a tunable complex phase shift $\delta = \delta_r + i \delta_i$ and a corresponding amplitude $e^{2i\delta} = e^{-2\delta_i} e^{2i\delta_r}$ appearing in front of the outgoing solution of the radial wavefunction of the square well potential $e^{-ik_{min}r} - e^{2i\delta} e^{+ik_{min}r}$ [92]. $e^{2i\delta}$ corresponds to a S_{SR} matrix element at short-range which probability $|S_{SR}|^2 = e^{-4\delta_i}$ is a number between 0 and 1 depending on δ_i and represents the probability for the flux going to the long-range region $r > r_{min}$. The loss probability p_{SR} is then defined as $p_{SR} = 1 - e^{-4\delta_i}$ so that $e^{-2\delta_i} \equiv \sqrt{1 - p_{SR}}$. We also note $\delta_r \equiv \delta_{SR}$.

The condition for full loss of the flux at short range is given by $p_{SR} = 1$ and gives $Z_{i,i}(r_{min}) = -i k_{min}$ for all diagonal elements. This is often called the universal regime since no resonances appear in the cross sections or rate coefficients [96, 92] and they are independent of the phase shifts δ_{SR} [97]. The results then become independent of the short-range interaction of the systems. The opposite condition for full reflection of the flux is given by $p_{SR} = 0$ and gives $Z(r_{min}) = k_{min}c/s$ which is the usual case for a square potential and depends on the tunable phase-shift δ_{SR} . With an adequate choice of $\delta_{SR} = -k_{min} r_{min}$ (modulo π), we can recover the infinite wall condition from Eq. (46). A number of $0 < p_{SR} < 1$ in between with $0 < \delta_{SR} < \pi$ describes an intermediate case where we can have both loss and reflection [96]. Actually, this can be a way to fit the theoretical results with experimental data [98, 99, 100] since the short-range potentials are not known generally.

The form of this initial tunable log-derivative is then flexible and can treat the possibility of loss at short-range in a phenomenological way. The complex log-derivative matrix provides a complex \mathbf{K} matrix and a \mathbf{S} matrix which is not a unitary matrix anymore. The difference of the sum of the $|S|^2$ matrix element for one channel with

unity provides the overall loss probability of this channel which translates into a loss cross section and a loss rate coefficient. This is an overall loss as we cannot determine each final state-to-state loss probabilities.

When describing ultracold collisions of reactive molecules, the universal regime condition at short-range $p_{SR} = 1$ is often chosen as we know nothing about the full potential energy surface. It is convenient since this condition is independent of the short-range interaction of the systems as mentioned above. It means that when the two molecules meet at short-range, the probability of reaction is one. Comparison with experimental data will eventually tell if one deviates from this regime or not. For the case of non-reactive molecules with a high density of Fano-Feshbach resonances around the collisional threshold [101, 102], this condition is also often chosen. In this case, it has been supposed that the molecules might form a molecule-molecule complex for a certain time. The higher the density of Fano-Feshbach resonances, the longer the lifetime of this forming complex. As a consequence, in this high density regime, it has been shown that the rate of two molecules being formed in the tetra-atomic complex is exactly the same as the rate of two molecules being destroyed at short-range with a full loss probability $p_{SR} = 1$ [102]. Subsequently, the complex can be destroyed by a collision with a third molecule, resulting in losses of the molecules. Recent experiments observed losses of non-reactive molecules in their absolute ground state for RbCs [103], NaK [104], and NaRb [105] molecules. Even though a direct observation of the forming complexes was not obtained, the hypothesis formulated in [101, 102] could be a possible explanation of the experimental molecular losses.

We end up with: (i) a long-range interaction from $r = r_{min}$ to $r = r_{max}$ and (ii) a short-range tunable boundary condition at $r = r_{min}$ which describes phenomenologically scattering phase-shifts and additional losses from short-range. To study the collision $\text{KRb} + \text{KRb} \rightarrow \text{K}_2 + \text{Rb}_2$, we will use the full loss (universal) condition at short-range $p_{SR} = 1$ so that $Z_{i,i}(r_{min}) = -i k_{min}$ for each diagonal elements.

7.2 Molecules in an electric field

We consider KRb molecules in their ground electronic state $^1\Sigma^+$ and their ground vibrational state $v = 0$. We do not take into account any spin structure as mentioned earlier. Then, only their rotational structure can change in a collision. The bare internal rotational states of a molecule are usual described by spherical harmonics $Y_{n_i}^{m_{n_i}}$ noted by the ket $|n_i m_{n_i}\rangle$ for molecule $i = 1, 2$. In this basis set, the rotational Hamiltonian is given by $\langle n_i m_{n_i} | h_{rot} | n'_i m'_{n_i} \rangle = B_{rot} n_i(n_i + 1) \delta_{n_i, n'_i} \delta_{m_{n_i}, m'_{n_i}}$ where B_{rot} is the rotational constant of the molecule. We take $B_{rot} = 1.113950$ GHz [87] for the fermionic $^{40}\text{K}^{87}\text{Rb}$ molecule and $B_{rot} = 1.095362$ GHz [106] for the bosonic $^{41}\text{K}^{87}\text{Rb}$ molecule. In an electric field, we add the Stark term given by the interaction $h_S = -\vec{d} \cdot \vec{E}$ between the permanent electric dipole moment \vec{d} of the molecule and an electric field $\vec{E} = E \vec{e}_Z$ taken along the OZ direction. In the basis set

$|n_i m_{n_i}\rangle$, the Stark term is written [107]:

$$\begin{aligned} \langle n_i m_{n_i} | h_S | n'_i m'_{n_i} \rangle &= -d E \delta_{m_{n_i}, m'_{n_i}} (-1)^{m_{n_i}} \sqrt{2n_i + 1} \sqrt{2n'_i + 1} \\ &\times \begin{pmatrix} n_i & 1 & n'_i \\ 0 & 0 & 0 \end{pmatrix} \begin{pmatrix} n_i & 1 & n'_i \\ -m_{n_i} & 0 & m'_{n_i} \end{pmatrix}. \end{aligned} \quad (92)$$

A permanent electric dipole moment \vec{d} is defined in the frame of the individual molecule, where the inter-atomic axis is chosen as quantization axis. We choose the convention that the orientation of the permanent dipole moment \vec{d} points from the negative to the positive distribution of charge [77]. The sign of the vector \vec{d} depends on the inter-atomic axis orientation in the frame of the individual molecule. This is an arbitrary choice but needs to be specified to avoid confusion. Here we assume that the inter-atomic axis is oriented from the lightest atom to the heaviest one [108] (for identical atoms of same mass, there is no electric dipole moment), as shown in Fig. 1 where the unit vector $\vec{\rho}_i/|\vec{\rho}_i|$ for molecule $i = 1, 2$ points from the lightest atom (represented by a small blue circle) to the heaviest one (represented by a big red circle). Using the above convention and the orientation of the inter-atomic axis, a positive vector \vec{d} would then mean that the negative distribution of charge is on the lightest atom while the positive distribution is on the heaviest one. A negative vector would mean the opposite. As an example, the permanent dipole moment \vec{d} for KRb is a positive vector with a magnitude of $d = 0.57$ D. It means that the negative distribution of charge is on the K atom while the positive one is on Rb, in the individual molecular frame. If we diagonalize the internal Hamiltonian matrix $h_i = h_{rot} + h_S$ for molecule $i = 1, 2$ in the basis set $|n_i m_{n_i}\rangle$, we get the corresponding eigenvectors (often called dressed states) $|\tilde{n}_i m_{n_i}\rangle$ for a given electric field, which are a linear combination of the bare state $|n_i m_{n_i}\rangle$. The quantum number m_{n_i} is conserved. The tilde corresponds to a certain admixture of different rotational quantum numbers due to the electric field but when $E \rightarrow 0$, the dressed states $|\tilde{n}_i m_{n_i}\rangle$ tend to the bare states $|n_i m_{n_i}\rangle$. The number of significantly admixed bare states increases with the magnitude of the electric field. The eigenenergies ε_{α_i} for molecule $i = 1, 2$ are shown in Fig. 5-a for the fermionic $^{40}\text{K}^{87}\text{Rb}$ molecule, for $E = [0 - 50]$ kV/cm where we used $n = [0 - 5]$ to insure convergence of the results. It is also useful to plot the induced dipole moment in the electric field direction in the space-fixed frame. The induced dipole moment is the mean value of the permanent dipole moment over the dressed state $|\tilde{n}_i m_{n_i}\rangle$ at a given electric field $E = E_0$:

$$d_{ind}(E_0) = \langle \tilde{n}_i m_{n_i} | \vec{d} \cdot \vec{e}_Z | \tilde{n}_i m_{n_i} \rangle \Big|_{E_0} = - \frac{d\varepsilon_{\alpha_i}}{dE} \Big|_{E_0}. \quad (93)$$

The sign of the induced dipole moment represents now the sign of the mean value of the permanent dipole moment for a given state in the direction of the electric field in the space-fixed frame. A positive sign represents a mean value pointing along the field while a negative sign represents a mean value pointing against the field. The induced dipole moments for different rotational states are shown in Fig. 5-b for the fermionic $^{40}\text{K}^{87}\text{Rb}$ molecule. The ground rotational state $|\tilde{0}, 0\rangle$ has a positive induced dipole moment growing in a monotonic way from 0 to $d = 0.57$ D. For

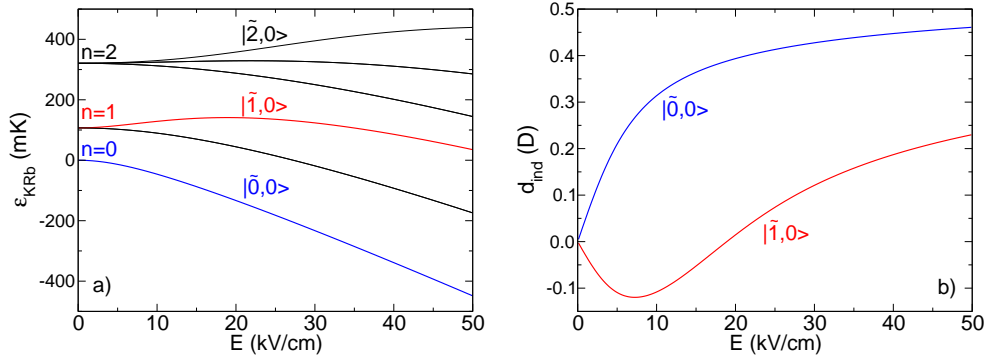


Figure 5: a) Energy of a fermionic $^{40}\text{K}^{87}\text{Rb}$ molecule as a function of an electric field for different internal states. b) Corresponding induced dipole moment d_{ind} in the direction of the electric field in the space-fixed frame for the $|\tilde{0},0\rangle$ and $|\tilde{1},0\rangle$ state.

the first excited state $|\tilde{1},0\rangle$ this is different. The induced dipole moment of $|\tilde{1},0\rangle$ is first negative from $E = 0$ to $E = 19$ kV/cm, with an increase in magnitude up to $E = 7.25$ kV/cm and a decrease after. Then it becomes positive at $E \geq 19$ kV/cm.

Finally, the energy of the combined initial dressed states $\epsilon_\alpha = \epsilon_{\alpha_1} + \epsilon_{\alpha_2}$ for two fermionic $^{40}\text{K}^{87}\text{Rb}$ molecules $i = 1, 2$ in an electric field, is shown in Fig. 6 as a function of the electric field. This gives an indication of the energy thresholds of the possible collisional states.

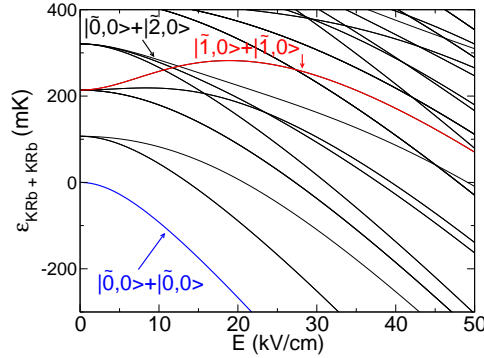


Figure 6: Energy of two separated fermionic $^{40}\text{K}^{87}\text{Rb}$ molecules as a function of an electric field. The blue (red) curve corresponds to the energy of two separated molecules in the ground (first excited) rotational state.

7.3 Collisions of molecules in an electric field

We use now a fixed collision energy $E_c = 500$ nK since this is a typical value reached in experiments of ultracold molecules. From the previous section, we know as well

the energy of the individual molecules as a function of an applied electric field. We use the dipole-dipole interaction in Eq. (88). The interaction varies as $-C_3/r^3$ and depends on the applied electric field. For the van der Waals interaction we use a value of $C_6 = 12636$ a.u. [94] for KRb. The molecules are identical and start in the same internal state so that they are indistinguishable. The partial waves used are $l = 1, 3, 5$ for the fermionic molecules and $l = 0, 2, 4$ for the bosonic ones. The initial quantum numbers for the individual molecules $i = 1, 2$ are $m_{n_i} = 0$. Those numbers are still good quantum numbers even in an electric field. The total $M_J = m_{n_1} + m_{n_2} + m_l = m'_{n_1} + m'_{n_2} + m'_l$ is conserved during the collision. As we start with $m_{n_1}, m_{n_2} = 0$, then $M_J = m_l$. At such an ultralow energy $E_c = 500$ nK, the most important partial wave is the first and lowest one. For fermions, the lowest partial wave quantum number is $l = 1$ (p-wave), so that $m_l = 0, \pm 1$. Then we restrict the calculation to $M_J = 0, \pm 1$. For bosons, the lowest partial wave quantum number is $l = 0$ (s-wave), so that $m_l = 0$, and then we restrict to $M_J = 0$. The corresponding diabatic and adiabatic energies for two fermionic $^{40}\text{K}^{87}\text{Rb}$ molecules in the ground rotational state $|\tilde{0}, 0\rangle$ at an electric field of $E = 5$ kV/cm are plotted in Fig. 7 as a function of r (see definition in Section 4). We selected the component $M_J = 0$ for this figure so that $m_l = 0$. At large distances, the energies tend to the energy of two separated molecules recovering the results in Fig. 6. At short distances, one can see the onset of the centrifugal terms characterized by the partial wave numbers $l = 1, 3, 5$ and the corresponding barriers. The diabatic curves are shown in black while the adiabatic ones are shown in red. The effect of the dipole-dipole coupling elements in Eq. (88) can be seen in this figure where the adiabatic energies differ from the diabatic ones.

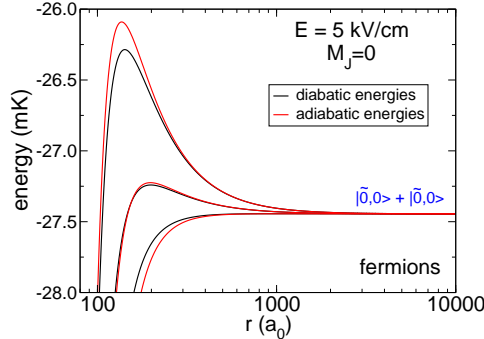


Figure 7: Diabatic (black) and adiabatic (red) energies for two fermionic $^{40}\text{K}^{87}\text{Rb}$ molecules in the ground rotational state at an electric field of $E = 5$ kV/cm.

We apply the quantum formalism that we have presented in this paper. This is what it is referred to as the close-coupling quantum calculation in the following. Starting with a boundary condition at $r_{min} = 10 a_0$, where a_0 is the Bohr radius, corresponding to a full loss condition at short-range, we propagate the log-derivative matrix \mathbf{Z} up to $r_{max} = 10000 a_0$. At this distance, we obtain the reactance, scattering and transition matrices $\mathbf{K}, \mathbf{S}, \mathbf{T}$, and finally the cross sections and rate coefficients. As we use a boundary condition with full loss at short-range, there are three collisional

processes possible: elastic, inelastic and loss processes. The loss processes mimic chemical reaction processes for reactive molecules. For non-reactive molecules, they would mimic the losses of two free molecules into a molecule-molecule complex, subsequently destroyed by a collision with a third molecule. In the following, we will call quenching processes the sum of inelastic and loss processes, that is everything that leads to molecular losses and compare with elastic processes. We present two cases: collisions of molecules (i) in the ground rotational state and (ii) in the first rotational excited state. For the former case, we also introduce an insightful model, a quantum threshold model, that semi-quantitatively explains the collisional results.

Molecules in the ground rotational state: enhancement of the loss rates

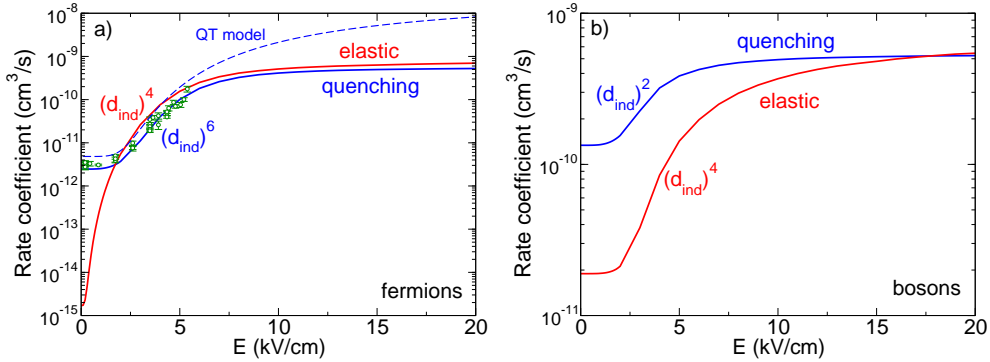


Figure 8: Rate coefficient as a function of an electric field for molecules in the ground rotational state $|\tilde{0}, 0\rangle$. Elastic (quenching) processes correspond to the red (blue) curves. The solid lines are the results from the close-coupling quantum formalism presented in this paper (see text for details). a): Fermionic $^{40}\text{K}^{87}\text{Rb} + ^{40}\text{K}^{87}\text{Rb}$ collisions. The data points (green circles) are the experimental results of Ref. [109]. The dashed line comes from a Quantum Threshold model [110], see Eq. (100). b): Bosonic $^{41}\text{K}^{87}\text{Rb} + ^{41}\text{K}^{87}\text{Rb}$ collisions.

We present in Fig. 8 the elastic (red) and quenching (blue) rate coefficients for fermions (Fig. 8-a) and bosons (Fig. 8-b) for two molecules in the ground rotational state $|\tilde{0}, 0\rangle$. The results were obtained using the close-coupling quantum calculation aforementioned. The energy threshold for the two molecules $|\tilde{0}, 0\rangle + |\tilde{0}, 0\rangle$ is shown in blue in Fig. 6. For fermions, experimental data of Ref. [109] are also included. Globally for both cases, the quenching rate dominates over the elastic rate or they have the same order of magnitude. This is a bad outcome for example for evaporative cooling purpose where elastic collisions have to be important while quenching collisions have to be negligible. Comparing fermions to bosons, similar behaviour is seen except that the bosonic rates are globally higher than the fermionic ones. This is expected from the parity of the l quantum numbers. For bosons, the l numbers are even and include the s-wave $l = 0$ curve, for which there is no centrifugal barrier (barrierless case). For fermions, the l numbers are odd and include the p-wave

$l = 1$ curve, for which there is a centrifugal barrier. In the former case, the particles approach each other easily without any barrier so that the rate is high while in the latter case, the particles approach less easily due to the presence of the p-wave centrifugal barrier.

Both rates increase with increasing electric field. They display the same behaviour as their induced dipole moment. When the electric field increases, the induced dipole moment increases monotonically (see Fig.5-b), so does the magnitude of the dipole-dipole interaction and then the rate coefficient. This can be explained by the fact that for fermions or bosons at ultralow energies, the main contribution to the rates comes from an attractive dipole-dipole interaction from the $m_l = 0$ component [110, 111]. When the electric field increases the dipole-dipole interaction becomes more and more attractive, favouring the meeting of molecules at short-range and then molecular losses.

Fermionic and bosonic elastic rates behave as d_{ind}^4 as predicted in Ref. [112]. Quenching rate coefficients have a strong dependence with increasing electric field and induced dipole moment. The fermionic quenching rates display a d_{ind}^6 behaviour as found in Ref. [110] while the bosonic quenching rates display a d_{ind}^2 one as found in Ref. [111].

A Quantum Threshold model

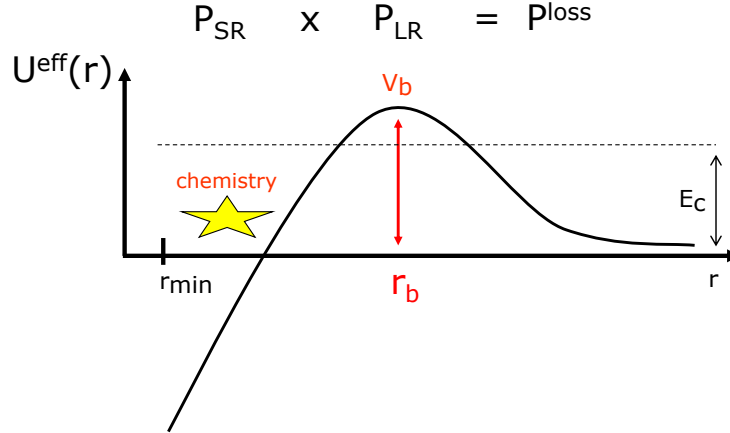


Figure 9: Basis of a simple Quantum Threshold model [110]. The incident particles have to overcome a barrier of height V_b at a position r_b at long-range. The probability to reach the short-range region is governed by the tunneling probability through the barrier and depends on the collision energy E_c and the height of the barrier, see Eq. (99).

The behaviour of the quenching rate coefficients can be found semi-quantitatively using a Quantum Threshold (QT) model [110]. The method consists in taking into account only the lowest channel curve of the initial colliding state corresponding to

the lowest partial wave quantum number. The energy of the two initial free particles is taken as reference. This curve is described by the interaction potential \mathcal{U}^{eff} :

$$\mathcal{U}^{eff}(r) = \mathcal{U}^{cent}(r) + \mathcal{U}^{int}(r) = \frac{\hbar^2 l(l+1)}{2m_{red}r^2} - \frac{C_s}{r^s}, \quad (94)$$

for an attractive interaction $-C_s/r^s$ with $s > 2$ and $C_s > 0$. The competition between the repulsive centrifugal potential and the attractive interaction creates a potential energy barrier for the incident colliding motion (or incident barrier), of height V_b at position r_b (see Fig. 9). The position and the height of the barrier are given by:

$$r_b = \left[\frac{m_{red} s C_s}{\hbar^2 l(l+1)} \right]^{1/(s-2)} \quad V_b = \frac{\hbar^2 l(l+1)}{2m_{red}r_b^2} - \frac{C_s}{r_b^s}. \quad (95)$$

In the case of a barrierless collisions ($l = 0$), one cannot define a position r_b and height V_b of a barrier. Instead the characteristic length and energy of the $-C_s/r^s$ interaction are taken in the model[111, 113]:

$$a_s = \left[\frac{2m_{red}C_s}{\hbar^2} \right]^{1/(s-2)} \quad E_s = \frac{\hbar^2}{2m_{red}a_s^2}. \quad (96)$$

The model simply uses two probabilities of collision: one at long-range and one at short-range. At long range, the two molecules see the incident barrier and tunnel through it. This is described by a long-range (tunneling) probability P_{LR} . The molecules enter then the short-range region, where they can chemically react or form a complex and be lost from the trap, with a probability P_{SR} . We will assume full probability of loss at short range so that $P_{SR} = 1$. Then the probability of loss is $P^{loss} = P_{SR} \times P_{LR} = P_{LR}$. To estimate the tunneling probability P_{LR} , we use:

(i) a classical Langevin model [114]: when $E_c \geq V_b$:

$$P_{LR}(E_c = V_b) = 1 \quad (97)$$

that is if the molecules have enough energy to overcome the barrier, the probability of passing above is one,

(ii) the form of the threshold laws for the loss probability (Eq. (87)): when $E_c \rightarrow 0$, the probability which is proportional to the cross section multiplied by $k^2 \sim E_c$ (see Eq. (73)) should obey:

$$P_{LR}(E_c) = \gamma E_c^{l+1/2}, \quad (98)$$

(iii) Eq. (97) to determine the constant γ in Eq. (98), so that $P_{LR}(E_c = V_b) = 1 = \gamma V_b^{l+1/2}$. Then we get $\gamma = 1/V_b^{l+1/2}$. Within the QT model, the total loss probability is:

$$P^{loss}(E_c) = \left(\frac{E_c}{V_b} \right)^{l+1/2}. \quad (99)$$

Replacing Eq. (99) into Eq. (73) leads to the quenching rate coefficient within the QT model for a given l, m_l :

$$\beta_{l, m_l}^{qu}(E_c) = \frac{\hbar^2 \pi}{\sqrt{2m_{red}^3}} \frac{E_c^l}{V_b^{l+1/2}} \Delta, \quad (100)$$

with $\Delta = 2$ if the particles are identical and indistinguishable and $\Delta = 1$ otherwise. This is a simple way to estimate the characteristics of loss collisions. Once we know the height of the barrier V_b we know how the rate coefficient scales. At zero electric field, the dominant interaction is the attractive van der Waals interaction with $s = 6$. For $l = 1$, $V_b = [8\hbar^2/54m_{red}^3C_6]^{1/2}$. For $l = 0$, $E_6 = \hbar^3/[8m_{red}^3C_6]^{1/2}$. In the electric field regime, $V_b = (25\hbar^6/108m_{red}^3) \times (d_{ind}^2/4\pi\epsilon_0)^{-2}$ for $l = 1$ and $E_4 = (15\hbar^6/16m_{red}^3) \times (d_{ind}^2/4\pi\epsilon_0)^{-2}$ for $l = 0$, where the characteristic interaction is $s = 4$, see Ref. [111] for more details. Inserting these expressions into Eq. (100), we see that the quenching rate behaves then as d_{ind}^6 and d_{ind}^2 for indistinguishable fermions ($l = 1$) and bosons ($l = 0$) respectively, and in general as $d_{ind}^{4(l+1/2)}$. For $l = 0$, the quenching rate coefficients are independent of the collision energy and hence of the temperature. For $l = 1$ and to get the rate coefficients as a function of the temperature T , one can replace E_c by $\langle E_c \rangle = 3k_B T/2$, the mean collision energy of a Maxwell-Boltzmann distribution.

The QT rate coefficient is shown in Fig. 9 as a dashed line for the fermionic case. It gives the proper scaling law and transition zone between the Van der Waals regime (where we took $l = 1, m_l = 0, \pm 1$) and the electric field regime (where we only took $l = 1, m_l = 0$). However it overestimates both quantum results and experimental data by about a factor of 2. This can be traced back in the classical Langevin criterion where we chose a unit probability when $E_c = V_b$. This is true in classical mechanics but in quantum mechanics, the colliding particles are described by a wave. Close to and at the top a barrier, a wave has a transmission probability but also a reflection probability, the sum of both being one. It implies that the transmission probability of the wave function is not equal to unity, in contrast with what is assumed by the classical Langevin model. This explains why the QT model gives an upper value of the quenching rates for fermions.

Comparing the QT quenching rates with the ones using the quantum formalism for different molecular systems of dipolar alkali molecules [111] provides the corrections to make for the model. The correction is a factor p of order of unity in front of Eq. (100). For $l = 1$, the corrections are $p = 0.53$ for the van der Waals regime and $p = 0.54$ for the electric field regime, while for $l = 0$ they are $p = 1.92$ and $p = 3.74$ respectively. Some of those values can also be found using a Quantum-Defect Theory (QDT) formalism [97, 115]. The QT model in Eq. (100) provides then an underestimating rate for the barrierless case $l = 0$ since the correction factor $p > 1$, while it gives an overestimating rate for the barrier case $l = 1$ since the correction factor $p < 1$. With the corrections of about 0.5 for $l = 1$ on this figure, one can see that the QT model will then agree with the numerical close-coupling quantum calculation and the experimental data.

Molecules in the first rotational excited state: suppression of the loss rates

What happens now if the molecules are prepared in the first excited rotational state $|\bar{1}, 0\rangle$? The corresponding rate coefficients [92] are presented in Fig. 10 using the

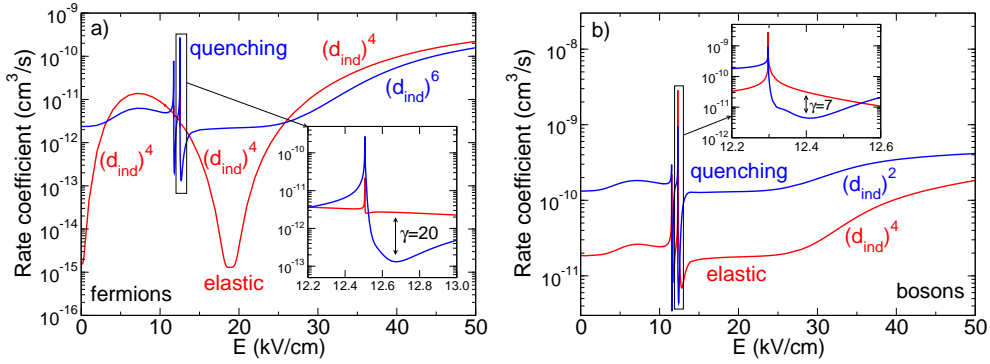


Figure 10: Rate coefficient as a function of an electric field for molecules in the first excited rotational state $|\tilde{1}, 0\rangle$. The solid lines are the results from the close-coupling quantum formalism presented in this paper (see text for details). a): Fermionic $^{40}\text{K}^{87}\text{Rb} + ^{40}\text{K}^{87}\text{Rb}$ collisions. b): Bosonic $^{41}\text{K}^{87}\text{Rb} + ^{41}\text{K}^{87}\text{Rb}$ collisions.

close-coupling quantum calculation. Globally, we found the same overall trend as for two molecules in the ground rotational state. The rates follow again the behaviour of the induced dipole moment as a function of the electric field: when $|d_{ind}|$ increases from $E = 0$ to $E = 7.25$ kV/cm and from $E = 19$ kV/cm, the rate increases, and inversely when it decreases from $E = 7.25$ kV/cm to $E = 19$ kV/cm, the rate decreases. We found again that the quenching rate behaves as d_{ind}^6 and d_{ind}^2 for fermions and bosons and that the elastic rate behaves as d_{ind}^4 .

The main interesting feature of Fig. 10 comes from the presence of sharply varying structures for the rates near $E^* \sim 12.5$ kV/cm and $E^* \sim 11.5$ kV/cm (two smoother ones appear near $E^* \sim 10.5$ kV/cm and $E^* \sim 27$ kV/cm but cannot be seen in the figure). This is in strike contrast with collisions of ground rotational states molecules. These features appear at the specific electric fields E^* where the energy threshold of other combined molecular states crosses the initial one $|\tilde{1}, 0\rangle + |\tilde{1}, 0\rangle$, shown in red in Fig. 6. Those states are for example the $|\tilde{0}, 0\rangle + |\tilde{2}, 0\rangle$ and the $|\tilde{0}, 0\rangle + |\tilde{2}, \pm 1\rangle$ for the two most prominent features respectively. Slightly below E^* , the quenching rate first increases when the electric field is increased, then above E^* , it suddenly drops. Eventually it gets back to a steady value far from E^* . In the region where the quenching rate is suppressed, the elastic rate remains quite high so that elastic processes are bigger than the loss processes, by a factor of $\gamma = 20$ for fermions and $\gamma = 7$ for bosons. The principle of this mechanism was originally explored in Ref. [116] for molecules without losses at short-range ($P_{SR} = 0$). We consider the initial colliding state of interest, here $|\tilde{1}, 0\rangle + |\tilde{1}, 0\rangle$ and we take the second prominent structure in the rates (insets of Fig. 10) as an example. When the electric field is increased starting from below E^* , the energy of the coupling state, $|\tilde{0}, 0\rangle + |\tilde{2}, 0\rangle$ in this example, approaches the one of the initial state $|\tilde{1}, 0\rangle + |\tilde{1}, 0\rangle$ from above. The effective potential curve ($\mathcal{U}^{eff}(r)$ in Eq. (38)) of the coupling state pushes the one of the initial state downward, due to the dipole-dipole coupling between the two channels. This results in lowering the curve of the initial

state, making it more attractive, hence favouring the molecules to come close to each other and react/be lost at short-range. The quenching rate is thus enhanced. When the electric field is further increased but from above E^* now, the energy of the coupling state lies below the one of the initial state. Its effective potential curve pushes upwards the one of the incident state. This results now in increasing the curve of the initial state, making it more repulsive, hence preventing the molecules to come close to each other. The quenching rate is suppressed.

Even though this mechanism has to be confirmed by experimental results, this is a promising way of suppressing molecular losses due to any reasons (inelastic collisions, chemical reactions, complex-forming losses). This is also promising to perform evaporative cooling of a dipolar gas since elastic processes are more efficient than quenching ones. In order to perform efficient evaporative cooling, a ratio of $\gamma \simeq 100$ has to be reached [4, 5], with perhaps a safer estimation using $\gamma \simeq 1000$. As described above, this is not the case for the KRb system where $\gamma \simeq 10$ so that evaporative cooling might not be an efficient method to further cool down the gas. However, the suppression of the quenching processes becomes more effective as the permanent electric dipole moment of the molecules increases [117]. For those molecules, the ratio γ can reach values of 1000 or more, so that the conditions for efficient evaporative cooling are fulfilled to further cool down dipolar gases and hopefully reach quantum degeneracy.

8 Conclusion and perspectives

In this paper we presented a time-independent quantum formalism to describe ultracold collisions of particles with internal structure, also accounting for the presence of an external field. It was shown, taking the dipolar KRb molecule as an example, how collisional properties can be tuned with an electric field, from enhancing the quenching rates to suppressing them.

Of course many other configurations could be engineered to control the molecules dynamics and could be implemented within the present formalism. For example, collisions of ultracold molecules in a confined geometry is possible by adding in the quantum formalism an external harmonic oscillator trap that can mimic the presence in an experiment of a one-dimensional optical lattice [54, 118]. For sufficiently high induced dipole moments and strong confinements, fermionic and bosonic collisional losses in two dimensions can be suppressed due to the side-by-side repulsive dipole-dipole interaction. In the particular case where the confinement of the lattice is not strong enough, only fermionic collisional losses can be suppressed due to appropriate selection rules related to the fermionic character of the system [54, 118]. The long-range ultracold dipolar physics is also quite general since experiments with ultracold magnetic dipolar molecules [119] lead to the same conclusions than for electric dipolar ones. In addition, any arbitrary electric or magnetic field with an arbitrary direction could also be added into the quantum formalism [71, 120], which can be interesting to control ultracold molecules that both possess electric and magnetic dipole moments. Another interesting tool of control is to employ electromagnetic waves and especially microwaves to control the rotational degree of

freedom of the molecules [121, 122, 123]. Finally, in addition to two-body collisions, three-body collisions [124, 125, 126] and more [60] can start to play a role for high density of the ultracold molecular cloud. The few- and many-body characters of the dipolar interactions can also start to reveal the increasing anisotropic complexity of the systems [127].

Treating all those additional possibilities goes beyond the scope of this paper. We introduced here only a small and simple part of the ultracold collision formalism. In the future, one could increase at will the versatility and the flexibility of the formalism to cover all possible configurations accessible in an experiment, certainly enabling the exploration of all new kinds of ultracold, ultra-controlled dynamics of molecules!

Appendix

Proof 1

Let's start with Eq. (39) (first equation) and its transpose (second equation) using the fact that \mathbf{U} is real and symmetric. Let's multiply by \mathbf{F}^t on the left for the first equation and by \mathbf{F} on the right for the second equation:

$$\begin{aligned} \mathbf{F}^t \times \{ \mathbf{D}^2 \mathbf{F} + \mathbf{U} \mathbf{F} \} &= 0 \\ \{ \mathbf{D}^2 \mathbf{F}^t + \mathbf{F}^t \mathbf{U} \} = 0 &\times \mathbf{F}. \end{aligned}$$

By retrieving both equations one gets:

$$\mathbf{F}^t (\mathbf{D}^2 \mathbf{F}) - (\mathbf{D}^2 \mathbf{F}^t) \mathbf{F} = 0$$

which implies:

$$\mathbf{D}[\mathbf{F}^t (\mathbf{D} \mathbf{F}) - (\mathbf{D} \mathbf{F}^t) \mathbf{F}] = 0$$

where $\mathbf{D} \equiv \mathbf{I} \frac{d}{dr}$. This means that the matrix $\mathbf{F}^t (\mathbf{D} \mathbf{F}) - (\mathbf{D} \mathbf{F}^t) \mathbf{F}$ is independent of r . Moreover at $r = r_{min}$, we took $\mathbf{F} = 0$ as mentioned by Eq. (46), so then:

$$\mathbf{F}^t (\mathbf{D} \mathbf{F}) - (\mathbf{D} \mathbf{F}^t) \mathbf{F} = 0 \quad \forall r.$$

By inserting Eq. (59) and its transpose into this expression, one gets:

$$(\mathbf{F}^{(1)} - \mathbf{K}^t \mathbf{F}^{(2)}) (\mathbf{F}'^{(1)} - \mathbf{F}'^{(2)} \mathbf{K}) - (\mathbf{F}'^{(1)} - \mathbf{K}^t \mathbf{F}'^{(2)}) (\mathbf{F}^{(1)} - \mathbf{F}^{(2)} \mathbf{K}) = 0$$

by factorizing the matrices $(\mathbf{N}^K)^t$ and \mathbf{N}^K , and by developing:

$$\begin{aligned} \mathbf{F}^{(1)} \mathbf{F}'^{(1)} - \mathbf{F}^{(1)} \mathbf{F}'^{(2)} \mathbf{K} - \mathbf{K}^t \mathbf{F}^{(2)} \mathbf{F}'^{(1)} + \mathbf{K}^t \mathbf{F}^{(2)} \mathbf{F}'^{(2)} \mathbf{K} \\ - \mathbf{F}'^{(1)} \mathbf{F}^{(1)} + \mathbf{F}'^{(1)} \mathbf{F}^{(2)} \mathbf{K} + \mathbf{K}^t \mathbf{F}'^{(2)} \mathbf{F}^{(1)} - \mathbf{K}^t \mathbf{F}'^{(2)} \mathbf{F}^{(2)} \mathbf{K} = 0. \end{aligned}$$

Using the fact that diagonal matrices commute, we finally get:

$$\mathbf{K}^t (\mathbf{F}'^{(2)} \mathbf{F}^{(1)} - \mathbf{F}^{(2)} \mathbf{F}'^{(1)}) = (\mathbf{F}^{(1)} \mathbf{F}'^{(2)} - \mathbf{F}'^{(1)} \mathbf{F}^{(2)}) \mathbf{K}$$

or in term of the Wronskian matrix:

$$\mathbf{K}^t \mathbf{W} = \mathbf{W} \mathbf{K}.$$

Since $\mathbf{W} = \mathbf{I}$ due to the $k_{\alpha'}^{-1/2}$ factors, this implies that $\mathbf{K}^t = \mathbf{K}$ so that \mathbf{K} is symmetric.

Proof 2

$$\begin{aligned}
\mathbf{Z} &= \mathbf{F}' \mathbf{F}^{-1} \\
&= \{\mathbf{F}'^{(1)} - \mathbf{F}'^{(2)} \mathbf{K}\} \mathbf{N}^K [\{\mathbf{F}^{(1)} - \mathbf{F}^{(2)} \mathbf{K}\} \mathbf{N}^K]^{-1} \\
&= \{\mathbf{F}'^{(1)} - \mathbf{F}'^{(2)} \mathbf{K}\} \mathbf{N}^K [\mathbf{N}^K]^{-1} \{\mathbf{F}^{(1)} - \mathbf{F}^{(2)} \mathbf{K}\}^{-1} \\
&= \{\mathbf{F}'^{(1)} - \mathbf{F}'^{(2)} \mathbf{K}\} \{\mathbf{F}^{(1)} - \mathbf{F}^{(2)} \mathbf{K}\}^{-1}.
\end{aligned}$$

Then:

$$\begin{aligned}
\mathbf{Z} \{\mathbf{F}^{(1)} - \mathbf{F}^{(2)} \mathbf{K}\} &= \{\mathbf{F}'^{(1)} - \mathbf{F}'^{(2)} \mathbf{K}\} \\
\mathbf{Z} \mathbf{F}^{(1)} - \mathbf{F}'^{(1)} &= \{\mathbf{Z} \mathbf{F}^{(2)} - \mathbf{F}'^{(2)}\} \mathbf{K} \\
\mathbf{K} &= \{\mathbf{Z} \mathbf{F}^{(2)} - \mathbf{F}'^{(2)}\}^{-1} \{\mathbf{Z} \mathbf{F}^{(1)} - \mathbf{F}'^{(1)}\}.
\end{aligned}$$

Proof 3

First as $r \rightarrow \infty$: $\mathbf{F}^\pm = -\mathbf{F}^{(2)} \pm i\mathbf{F}^{(1)}$. This implies $\mathbf{F}^{(1)} = (\mathbf{F}^+ - \mathbf{F}^-)/2i$ and $\mathbf{F}^{(2)} = -(\mathbf{F}^+ + \mathbf{F}^-)/2$.

Then:

$$\begin{aligned}
\mathbf{F} &= \mathbf{F}^{(1)} \mathbf{A} + \mathbf{F}^{(2)} \mathbf{B} \\
&= \{(\mathbf{F}^+ - \mathbf{F}^-)/2i\} \mathbf{A} - \{(\mathbf{F}^+ + \mathbf{F}^-)/2\} \mathbf{B} \\
&= (\mathbf{F}^+ \mathbf{A})/2i - (\mathbf{F}^- \mathbf{A})/2i - (\mathbf{F}^+ \mathbf{B})/2 - (\mathbf{F}^- \mathbf{B})/2 \\
&= \mathbf{F}^- [-(\mathbf{B} - i\mathbf{A})/2] + \mathbf{F}^+ [-(\mathbf{B} + i\mathbf{A})/2] \\
&\equiv \mathbf{F}^- \mathbf{A}' + \mathbf{F}^+ \mathbf{B}'.
\end{aligned}$$

From that we identify:

$$\begin{aligned}
\mathbf{A}' &= i/2 (\mathbf{A} + i\mathbf{B}) & \mathbf{B}' &= -i/2 (\mathbf{A} - i\mathbf{B}) \\
\mathbf{A} &= -i(\mathbf{A}' - \mathbf{B}') & \mathbf{B} &= -(\mathbf{A}' + \mathbf{B}').
\end{aligned}$$

We know from Eq. (64) and Eq. (65) that:

$$\begin{aligned}
\mathbf{S} &\equiv -\mathbf{B}' \mathbf{A}'^{-1} \\
&= [\mathbf{A} - i\mathbf{B}] [\mathbf{A} + i\mathbf{B}]^{-1} \\
&= [(\mathbf{I} - i\mathbf{B} \mathbf{A}^{-1}) \mathbf{A}] [(\mathbf{I} + i\mathbf{B} \mathbf{A}^{-1}) \mathbf{A}]^{-1} \\
&= (\mathbf{I} - i\mathbf{B} \mathbf{A}^{-1}) \mathbf{A} \mathbf{A}^{-1} (\mathbf{I} + i\mathbf{B} \mathbf{A}^{-1})^{-1} \\
&= (\mathbf{I} + i\mathbf{K}) (\mathbf{I} - i\mathbf{K})^{-1}
\end{aligned}$$

where we used $\mathbf{K} \equiv -\mathbf{B} \mathbf{A}^{-1}$ from Eq. (59) and Eq. (60). The matrix $\mathbf{M} = \mathbf{I} + i\mathbf{K}$ is what is called a normal matrix since \mathbf{M} and \mathbf{M}^\dagger commute ($\mathbf{M} \mathbf{M}^\dagger = \mathbf{M}^\dagger \mathbf{M}$, easy to show using the fact that \mathbf{K} is real and symmetric). Then \mathbf{M} and \mathbf{M}^\dagger can be expressed by $\mathbf{P} \mathbf{D}_M \mathbf{P}^{-1}$ and $\mathbf{P} \mathbf{D}_{M^\dagger} \mathbf{P}^{-1}$ with the same invertible matrix \mathbf{P} . $\mathbf{D}_{M, M^\dagger}$

are diagonal matrices with different complex eigenvalues since \mathbf{M} is not a hermitian matrix. Then:

$$\begin{aligned}
\mathbf{M} [\mathbf{M}^\dagger]^{-1} &= \mathbf{P} \mathbf{D}_M \mathbf{P}^{-1} [\mathbf{P} \mathbf{D}_{M^\dagger} \mathbf{P}^{-1}]^{-1} \\
&= \mathbf{P} \mathbf{D}_M \mathbf{P}^{-1} \mathbf{P} \mathbf{D}_{M^\dagger}^{-1} \mathbf{P}^{-1} = \mathbf{P} \mathbf{D}_M \mathbf{D}_{M^\dagger}^{-1} \mathbf{P}^{-1} \\
&= \mathbf{P} \mathbf{D}_{M^\dagger}^{-1} \mathbf{D}_M \mathbf{P}^{-1} = \mathbf{P} \mathbf{D}_{M^\dagger}^{-1} \mathbf{P}^{-1} \mathbf{P} \mathbf{D}_M \mathbf{P}^{-1} \\
&= [\mathbf{P} \mathbf{D}_{M^\dagger} \mathbf{P}^{-1}]^{-1} \mathbf{P} \mathbf{D}_M \mathbf{P}^{-1} \\
&= [\mathbf{M}^\dagger]^{-1} \mathbf{M}
\end{aligned}$$

so that one also have $\mathbf{S} = \{\mathbf{I} + i\mathbf{K}\} \{\mathbf{I} - i\mathbf{K}\}^{-1} = \{\mathbf{I} - i\mathbf{K}\}^{-1} \{\mathbf{I} + i\mathbf{K}\}$. Because both matrices commute, we can safely write the expression as:

$$\mathbf{S} = \frac{\mathbf{I} + i\mathbf{K}}{\mathbf{I} - i\mathbf{K}}.$$

We also know that:

$$\begin{aligned}
\mathbf{N}^K &\equiv \mathbf{A} = -i(\mathbf{A}' - \mathbf{B}') \\
&= -i(\mathbf{I} - \mathbf{B}' \mathbf{A}'^{-1}) \mathbf{A}' \\
&= -i(\mathbf{I} + \mathbf{S}) \mathbf{N}^S,
\end{aligned}$$

and inversely:

$$\begin{aligned}
\mathbf{N}^S &\equiv i/2 (\mathbf{A} + i\mathbf{B}) \\
&= i/2 (\mathbf{I} + i\mathbf{B} \mathbf{A}^{-1}) \mathbf{A} \\
&= i/2 (\mathbf{I} - i\mathbf{K}) \mathbf{N}^K.
\end{aligned}$$

If we use the forms in Eq. (60) or Eq. (65), by developing we can find:

$$\begin{aligned}
\mathbf{F}^K &= \{\mathbf{F}^{(1)} - \mathbf{F}^{(2)} \mathbf{K}\} \\
&= \{\mathbf{F}^- - \mathbf{F}^+ \{\mathbf{I} + i\mathbf{K}\} \{\mathbf{I} - i\mathbf{K}\}^{-1}\} \{-\{\mathbf{I} - i\mathbf{K}\}\} / 2i \\
&= \{\mathbf{F}^- - \mathbf{F}^+ \mathbf{S}\} \{-\{\mathbf{I} - i\mathbf{K}\}\} / 2i \\
&= \mathbf{F}^S \{-\{\mathbf{I} - i\mathbf{K}\}\} / 2i \\
&= \mathbf{F}^S \mathbf{N}^S (\mathbf{N}^K)^{-1},
\end{aligned}$$

so that we check that $\mathbf{F}^K \mathbf{N}^K = \mathbf{F}^S \mathbf{N}^S = \mathbf{F}$.

Proof 4

$$\mathbf{S}^t = \left[\frac{\mathbf{I} + i\mathbf{K}}{\mathbf{I} - i\mathbf{K}} \right]^t = \frac{\mathbf{I} + i\mathbf{K}^t}{\mathbf{I} - i\mathbf{K}^t} = \mathbf{S}$$

so that \mathbf{S} is symmetric.

$$\mathbf{S}^\dagger = \left[\frac{\mathbf{I} + i\mathbf{K}}{\mathbf{I} - i\mathbf{K}} \right]^\dagger = \frac{\mathbf{I} - i\mathbf{K}^\dagger}{\mathbf{I} + i\mathbf{K}^\dagger} = \mathbf{S}^{-1}$$

so that \mathbf{S} is unitary.

References

- [1] S. Chu, *Nobel Lecture: The manipulation of neutral particles*, Rev. Mod. Phys. **70**, 685 (1998).
- [2] C. N. Cohen-Tannoudji, *Nobel Lecture: Manipulating atoms with photons*, Rev. Mod. Phys. **70**, 707 (1998).
- [3] W. D. Phillips, *Nobel Lecture: Laser cooling and trapping of neutral atoms*, Rev. Mod. Phys. **70**, 721 (1998).
- [4] E. A. Cornell and C. E. Wieman, *Nobel Lecture: Bose-Einstein condensation in a dilute gas, the first 70 years and some recent experiments*, Rev. Mod. Phys. **74**, 875 (2002).
- [5] W. Ketterle, *Nobel lecture: When atoms behave as waves: Bose-Einstein condensation and the atom laser*, Rev. Mod. Phys. **74**, 1131 (2002).
- [6] M. Lewenstein, A. Sanpera, V. Ahufinger, B. Damski, A. Sen(De), and U. Sen, *Ultracold atomic gases in optical lattices: mimicking condensed matter physics and beyond*, Adv. Phys. **56**, 243 (2007).
- [7] I. Bloch, J. Dalibard, and W. Zwerger, *Many-body physics with ultracold gases*, Rev. Mod. Phys. **80**, 885 (2008).
- [8] M. Baranov, *Theoretical progress in many-body physics with ultracold dipolar gases*, Phys. Rep. **464**, 71 (2008).
- [9] E. S. Shuman, J. F. Barry, and D. DeMille, *Laser cooling of a diatomic molecule*, Nature **467**, 820 (2010).
- [10] M. Schnell and G. Meijer, *Cold Molecules: Preparation, applications, and challenges*, Angew. Chem. Int. Ed. **48**, 6010 (2009).
- [11] O. Dulieu and C. Gabbanini, *The formation and interactions of cold and ultracold molecules: new challenges for interdisciplinary physics*, Rep. Prog. Phys. **72**, 086401 (2009).
- [12] N. R. Hutzler, H.-I. Lu, and J. M. Doyle, *The Buffer Gas Beam: An intense, cold, and slow source for atoms and molecules*, Chem. Rev. **112**, 4803 (2012).
- [13] S. Y. T. van de Meerakker, H. L. Bethlem, N. Vanhaecke, and G. Meijer, *Manipulation and control of molecular beams*, Chem. Rev. **112**, 4828 (2012).
- [14] E. Narevicius and M. G. Raizen, *Toward cold chemistry with magnetically decelerated supersonic beams*, Chem. Rev. **112**, 4879 (2012).
- [15] M. Zeppenfeld, B. G. U. Englert, R. Glöckner, A. Prehn, M. Mielenz, C. Sommer, L. D. van Buuren, M. Motsch, and G. Rempe, *Sisyphus cooling of electrically trapped polyatomic molecules*, Nature **491**, 570 (2012).
- [16] H. R. Thorsheim, J. Weiner, and P. S. Julienne, *Laser-induced photoassociation of ultracold sodium atoms*, Phys. Rev. Lett. **58**, 2420 (1987).
- [17] A. Fioretti, D. Comparat, A. Crubellier, O. Dulieu, F. Masnou-Seeuws, and P. Pillet, *Formation of cold Cs_2 molecules through photoassociation*, Phys. Rev. Lett. **80**, 4402 (1998).

- [18] J. Weiner, V. S. Bagnato, S. Zilio, and P. S. Julienne, *Experiments and theory in cold and ultracold collisions*, Rev. Mod. Phys. **71**, 1 (1999).
- [19] K. M. Jones, E. Tiesinga, P. D. Lett, and P. S. Julienne, *Ultracold photoassociation spectroscopy: long-range molecules and atomic scattering*, Rev. Mod. Phys. **78**, 483 (2006).
- [20] J. Ulmanis, J. Deiglmayr, M. Repp, R. Wester, and M. Weidemüller, *Ultracold molecules formed by photoassociation: heteronuclear dimers, inelastic collisions, and interactions with ultrashort laser pulses*, Chem. Rev. **112**, 4890 (2012).
- [21] T. Köhler, K. Góral, and P. S. Julienne, *Production of cold molecules via magnetically tunable Feshbach resonances*, Rev. Mod. Phys. **78**, 1311 (2006).
- [22] C. Chin, R. Grimm, P. Julienne, and E. Tiesinga, *Feshbach resonances in ultracold gases*, Rev. Mod. Phys. **82**, 1225 (2010).
- [23] K. Bergmann, H. Theuer, and B. W. Shore, *Coherent population transfer among quantum states of atoms and molecules*, Rev. Mod. Phys. **70**, 1003 (1998).
- [24] K.-K. Ni, S. Ospelkaus, M. H. G. de Miranda, A. Pe'er, B. Neyenhuis, J. J. Zirbel, S. Kotochigova, P. S. Julienne, D. S. Jin, and J. Ye, *A high phase-space-density gas of polar molecules*, Science **322**, 231 (2008).
- [25] J. G. Danzl, E. Haller, M. Gustavsson, M. J. Mark, R. Hart, N. Bouloufa, O. Dulieu, H. Ritsch, and H.-C. Nägerl, *Quantum gas of deeply bound ground state molecules*, Science **321**, 1062 (2008).
- [26] C. P. Koch and M. Shapiro, *Coherent control of ultracold photoassociation*, Chem. Rev. **112**, 4928 (2012).
- [27] K. Bergmann, N. V. Vitanov, and B. W. Shore, *Perspective: stimulated Raman adiabatic passage: the status after 25 years*, J. Chem. Phys. **142**, 170901 (2015).
- [28] R. V. Krems, *Molecules near absolute zero and external field control of atomic and molecular dynamics*, Int. Rev. Phys. Chem. **24**, 99 (2005).
- [29] R. V. Krems, *Cold controlled chemistry*, Phys. Chem. Chem. Phys. **10**, 4079 (2008).
- [30] G. Quémener and P. S. Julienne, *Ultracold molecules under control!*, Chem. Rev. **112**, 4949 (2012).
- [31] M. Leshchko, R. V. Krems, J. M. Doyle, and S. Kais, *Manipulation of molecules with electromagnetic fields*, Mol. Phys. **111**, 1648 (2013).
- [32] L. D. Carr, D. DeMille, R. V. Krems, and J. Ye, *Cold and ultracold molecules: science, technology and applications*, New J. Phys. **11**, 055049 (2009).
- [33] A. Micheli, G. Pupillo, H. P. Büchler, and P. Zoller, *Cold polar molecules in two-dimensional traps: tailoring interactions with external fields for novel quantum phases*, Phys. Rev. A **76**, 043604 (2007).

- [34] A. V. Gorshkov, S. R. Manmana, G. Chen, J. Ye, E. Demler, M. D. Lukin, and A. M. Rey, *Tunable superfluidity and quantum magnetism with ultracold polar molecules*, Phys. Rev. Lett. **107**, 115301 (2011).
- [35] M. A. Baranov, M. Dalmonte, G. Pupillo, and P. Zoller, *Condensed matter theory of dipolar quantum gases*, Chem. Rev. **112**, 5012 (2012).
- [36] M. L. Wall, K. R. A. Hazzard, and A.-M. Rey, *Quantum magnetism with ultracold molecules*, Chapter 1 in From atomic to mesoscale: the role of quantum coherence in systems of various complexities. Edited by S. A. Malinovskaya, I. Novikova, World Scientific Publishing Co **1406**, 4758 (2014).
- [37] D. DeMille, *Quantum computation with trapped polar molecules*, Phys. Rev. Lett. **88**, 067901 (2002).
- [38] S. F. Yelin, K. Kirby, and R. Côté, *Schemes for robust quantum computation with polar molecules*, Phys. Rev. A **74**, 050301 (2006).
- [39] M. Karra, K. Sharma, B. Friedrich, S. Kais, and D. Herschbach, *Prospects for quantum computing with an array of ultracold polar paramagnetic molecules*, J. Chem. Phys. **144**, 094301 (2016).
- [40] E. A. Hinds, *Testing time reversal symmetry using molecules*, Phys. Scr. **1997**, 34 (1997).
- [41] M. R. Tarbutt, J. J. Hudson, B. E. Sauer, and E. A. Hinds, *Preparation and manipulation of molecules for fundamental physics tests*, Chapter 15 in Cold molecules: theory, experiments, applications. Edited by R. Krems, B. Friedrich, B. and W. C. Stwalley, CRC Press, 69 (2009).
- [42] M. L. González-Martínez, O. Dulieu, P. Larrégaray, and L. Bonnet, *Statistical product distributions for ultracold reactions in external fields*, Phys. Rev. A **90**, 052716 (2014).
- [43] T. V. Tscherbul and R. V. Krems, *Tuning bimolecular chemical reactions by electric fields*, Phys. Rev. Lett. **115**, 023201 (2015).
- [44] P. F. Weck and N. Balakrishnan, *Importance of long-range interactions in chemical reactions at cold and ultracold temperatures*, Int. Rev. Phys. Chem. **25**, 283 (2006).
- [45] J. M. Hutson and P. Soldán, *Molecular collisions in ultracold atomic gases*, Int. Rev. Phys. Chem. **26**, 1 (2007).
- [46] G. Quémener, N. Balakrishnan, and A. Dalgarno, *Inelastic collisions and chemical reactions of molecules at ultracold temperatures*, Chapter 3 in Cold molecules: theory, experiments, applications. Edited by R. Krems, B. Friedrich, B. and W. C. Stwalley, CRC Press, 3 (2009).
- [47] B. Brandsen and C. Joachain, *Physics of atoms and molecules*, Addison-Wesley, 2003.
- [48] C. Cohen-Tannoudji, B. Diu, and F. Laloë, *Mécanique quantique*, Hermann, 1997.
- [49] H. Friedrich, *Theoretical atomic physics, third edition*, Springer, 2005.

- [50] L. D. Landau and L. M. Lifshitz, *Quantum mechanics (non-relativistic theory)*, Butterworth Heinemann, 1958.
- [51] M. S. Child, *Molecular collision theory*, Dover Publications, 1996.
- [52] P. W. Atkins and R. S. Friedman, *Molecular quantum mechanics*, Oxford University Press, 2005.
- [53] J.-M. Launay, *Collisions moléculaires, cours du DEA Physique, option "physique atomique et moléculaire"*, Université de Rennes 1.
- [54] G. Quémener and J. L. Bohn, *Dynamics of ultracold molecules in confined geometry and electric field*, Phys. Rev. A **83**, 012705 (2011).
- [55] S. Grishkevich, S. Sala and A. Saenz, *Theoretical description of two ultracold atoms in finite three-dimensional optical lattices using realistic interatomic interaction potentials*, Phys. Rev. A **84**, 062710 (2011).
- [56] R. C. Whitten and F. T. Smith, *Symmetric representation for three-body problems. II. Motion in space*, J. Math. Phys. **9**, 1103 (1968).
- [57] B. R. Johnson, *The quantum dynamics of three particles in hyperspherical coordinates*, J. Chem. Phys. **79**, 1916 (1983).
- [58] R. T. Pack and G. A. Parker, *Quantum reactive scattering in three dimensions using hyperspherical (APH) coordinates. Theory*, J. Chem. Phys. **87**, 3888 (1987).
- [59] J. M. Launay and M. Le Dourneuf, *Hyperspherical close-coupling calculation of integral cross sections for the reaction $H+H_2 \rightarrow H_2+H$* , Chem. Phys. Lett. **163**, 178 (1989).
- [60] S. T. Rittenhouse, J. von Stecher, J. P. DIncao, N. P. Mehta, and C. H. Greene, *The hyperspherical four-fermion problem*, J. Phys. B: At. Mol. Opt. Phys. **44**, 172001 (2011).
- [61] C. F. Curtiss, *The quantum mechanics of collisions between diatomic molecules*, J. Chem. Phys. **21**, 2045 (1953).
- [62] K. Takayanagi, *The theory of collisions between two diatomic molecules*, Prog. Theor. Phys. **11**, 557 (1954).
- [63] A. M. Arthurs and A. Dalgarno, *The theory of scattering by a rigid rotator*, Proc. Roy. Soc. **256**, 540 (1960).
- [64] R. T. Pack, *Space-fixed vs body-fixed axes in atom-diatom molecule scattering. Sudden approximations*, J. Chem. Phys. **60**, 633 (1974).
- [65] S. Green, *Rotational excitation in H_2-H_2 collisions: close-coupling calculations*, J. Chem. Phys. **62**, 2271 (1975).
- [66] M. H. Alexander and A. E. DePristo, *Symmetry considerations in the quantum treatment of collisions between two diatomic molecules*, J. Chem. Phys. **66**, 2166 (1977).
- [67] J. M. Launay, *Body-fixed formulation of rotational excitation: exact and centrifugal decoupling results for $CO-He$* , J. Phys. B: At. Mol. Opt. Phys. **9**, 1823 (1976).

- [68] T. G. Heil, S. Green, and D. J. Kouri, *The coupled states approximation for scattering of two diatoms*, J. Chem. Phys. **68**, 2562 (1978).
- [69] K. Takayanagi, *The production of rotational and vibrational transitions in encounters between molecules*, Adv. At. Mol. Phys. **1**, 149 (1965).
- [70] G. Zarur and H. Rabitz, *Effective potential formulation of molecule-molecule collisions with application to H_2-H_2* , J. Chem. Phys. **60**, 2057 (1974).
- [71] G. Quémener and J. L. Bohn, *Ultracold molecular collisions in combined electric and magnetic fields*, Phys. Rev. A **88**, 012706 (2013).
- [72] T. V. Tscherbul and A. Dalgarno, *Quantum theory of molecular collisions in a magnetic field: Efficient calculations based on the total angular momentum representation*, J. Chem. Phys. **133**, 184104 (2010).
- [73] T. V. Tscherbul, *Total-angular-momentum representation for atom-molecule collisions in electric fields*, Phys. Rev. A **85**, 052710 (2012).
- [74] B. R. Johnson, *The multichannel log-derivative method for scattering calculations*, J. Comp. Phys. **13**, 445 (1973).
- [75] B. R. Johnson, *The renormalized Numerov method applied to calculating bound states of the coupled-channel Schrödinger equation*, J. Chem. Phys. **69**, 4678 (1978).
- [76] D. E. Manolopoulos, *An improved log derivative method for inelastic scattering*, J. Chem. Phys. **85**, 6425 (1986).
- [77] A. J. Stone, *The theory of intermolecular forces*, Oxford University Press, 1996.
- [78] J. M. Hutson, *Coupled channel methods for solving the bound-state Schrödinger equation*, Comput. Phys. Commun. **84**, 1 (1994).
- [79] M. Abramowitz and I. Stegun, *Handbook of mathematical functions with formulas, graphs, and mathematical tables*, United States Department of Commerce, National Bureau of Standards, 1964.
- [80] J. P. Burke, Jr., *Theoretical investigation of cold alkali atom collisions*, PhD thesis, University of Colorado, Boulder (USA), 1999.
- [81] T. V. Tscherbul, Y. V. Suleimanov, V. Aquilanti, and R. V. Krems, *Magnetic field modification of ultracold molecule molecule collisions*, New J. Phys. **11**, 055021 (2009).
- [82] C. J. Pethick and H. Smith, *Bose–Einstein condensation in dilute gases*, Cambridge University Press, 2001.
- [83] L. P. Pitaevskii and S. Stringari, *Bose–Einstein condensation*, Oxford: Clarendon Press, 2003.
- [84] H. R. Sadeghpour, J. L. Bohn, M. J. Cavagnero, B. D. Esry, I. I. Fabrikant, J. H. Macek, and A. R. P. Rau, *Collisions near threshold in atomic and molecular physics*, J. Phys. B: At. Mol. Opt. Phys. **33**, 93 (2000).
- [85] J. M. Hutson, *Theory of cold atomic and molecular collisions*, Chapter 1 in Cold molecules: theory, experiments, applications. Edited by R. Krems, B. Friedrich, B. and W. C. Stwalley, CRC Press, 3 (2009).

- [86] E. P. Wigner, *On the behavior of cross sections near thresholds*, Phys. Rev. **73**, 1002 (1948).
- [87] S. Ospelkaus, K.-K. Ni, G. Quéméner, B. Neyenhuis, D. Wang, M. H. G. de Miranda, J. L. Bohn, J. Ye, and D. S. Jin, *Controlling the hyperfine state of rovibronic ground-state polar molecules*, Phys. Rev. Lett. **104**, 030402 (2010).
- [88] P. S. Żuchowski and J. M. Hutson, *Reactions of ultracold alkali-metal dimers*, Phys. Rev. A **81**, 060703 (2010).
- [89] J. N. Byrd, J. A. Montgomery, and R. Côté, *Structure and thermochemistry of K_2Rb , KRb_2 , and K_2Rb_2* , Phys. Rev. A **82**, 010502 (2010).
- [90] E. R. Meyer and J. L. Bohn, *Product-state control of bi-alkali-metal chemical reactions*, Phys. Rev. A **82**, 042707 (2010).
- [91] J. N. Byrd, J. A. Montgomery, and R. Côté, *Long-range forces between polar alkali-metal diatoms aligned by external electric fields*, Phys. Rev. A **86**, 032711 (2012).
- [92] G. Wang and G. Quéméner, *Tuning ultracold collisions of excited rotational dipolar molecules*, New J. Phys. **17**, 035015 (2015).
- [93] S. Kotochigova, *Dispersion interactions and reactive collisions of ultracold polar molecules*, New J. Phys. **12**, 073041 (2010).
- [94] M. Lepers, R. Vexiau, M. Aymar, N. Bouloufa-Maafa, and O. Dulieu, *Long-range interactions between polar alkali-metal diatoms in external electric fields*, Phys. Rev. A **88**, 032709 (2013).
- [95] P. S. Zuchowski, M. Kosicki, M. Kodrycka, and P. Soldán, *Van der Waals coefficients for systems with ultracold polar alkali-metal molecules*, Phys. Rev. A **87**, 022706 (2013).
- [96] Z. Idziaszek, G. Quéméner, J. L. Bohn, and P. S. Julienne, *Simple quantum model of ultracold polar molecule collisions*, Phys. Rev. A **82**, 020703 (2010).
- [97] Z. Idziaszek and P. S. Julienne, *Universal Rate Constants for reactive collisions of ultracold molecules*, Phys. Rev. Lett. **104**, 113202 (2010).
- [98] M. Bishof, M. J. Martin, M. D. Swallows, C. Benko, Y. Lin, G. Quéméner, A. M. Rey, and J. Ye, *Inelastic collisions and density-dependent excitation suppression in a ^{87}Sr optical lattice clock*, Phys. Rev. A **84**, 052716 (2011).
- [99] A. D. Ludlow, N. D. Lemke, J. A. Sherman, C. W. Oates, G. Quéméner, J. von Stecher, and A. M. Rey, *Cold-collision-shift cancellation and inelastic scattering in a Yb optical lattice clock*, Phys. Rev. A **84**, 052724 (2011).
- [100] K. Jachymski, M. Michał, P. S. Julienne, and Z. Idziaszek, *Quantum theory of reactive collisions for $1/r^n$ potentials*, Phys. Rev. Lett. **110**, 213202 (2013).
- [101] M. Mayle, B. P. Ruzic, and J. L. Bohn, *Statistical aspects of ultracold resonant scattering*, Phys. Rev. A **85**, 062712 (2012).
- [102] M. Mayle, G. Quéméner, B. P. Ruzic, and J. L. Bohn, *Scattering of ultracold molecules in the highly resonant regime*, Phys. Rev. A **87**, 012709 (2013).

- [103] T. Takekoshi, L. Reichsöllner, A. Schindewolf, J. M. Hutson, C. R. Le Sueur, O. Dulieu, F. Ferlaino, R. Grimm, and H.-C. Nägerl, *Ultracold dense samples of dipolar RbCs molecules in the rovibrational and hyperfine ground state*, Phys. Rev. Lett. **113**, 205301 (2014).
- [104] J. W. Park, S. A. Will, and M. W. Zwierlein, *Ultracold dipolar gas of fermionic $^{23}\text{Na}^{40}\text{K}$ molecules in their absolute ground state*, Phys. Rev. Lett. **114**, 205302 (2015).
- [105] M. Guo, B. Zhu, B. Lu, X. Ye, F. Wang, R. Vexiau, N. Bouloufa-Maafa, G. Quéméner, O. Dulieu, and D. Wang, *Creation of an ultracold gas of ground-state dipolar $^{23}\text{Na}^{87}\text{Rb}$ molecules*, Phys. Rev. Lett. **116**, 205303 (2016).
- [106] K. Aikawa, D. Akamatsu, M. Hayashi, K. Oasa, J. Kobayashi, P. Naidon, T. Kishimoto, M. Ueda, and S. Inouye, *Coherent Transfer of Photoassociated Molecules into the Rovibrational Ground State*, Phys. Rev. Lett. **105**, 203001 (2010).
- [107] J. L. Bohn, *Electric dipoles at ultralow temperatures*, Chapter 2 in Cold molecules: theory, experiments, applications. Edited by R. Krems, B. Friedrich, B. and W. C. Stwalley, CRC Press, 3 (2009).
- [108] M. Aymar and O. Dulieu, *Calculation of accurate permanent dipole moments of the lowest $^1, 3\Sigma^+$ states of heteronuclear alkali dimers using extended basis sets*, J. Chem. Phys. **122**, 204302 (2005).
- [109] K.-K. Ni, S. Ospelkaus, D. Wang, G. Quéméner, B. Neyenhuis, M. H. G. de Miranda, J. L. Bohn, D. S. Jin, and J. Ye, *Dipolar collisions of polar molecules in the quantum regime*, Nature **464**, 1324 (2010).
- [110] G. Quéméner and J. L. Bohn, *Strong dependence of ultracold chemical rates on electric dipole moments*, Phys. Rev. A **81**, 022702 (2010).
- [111] G. Quéméner, J. L. Bohn, A. Petrov, and S. Kotochigova, *Universalities in ultracold reactions of alkali-metal polar molecules*, Phys. Rev. A **84**, 062703 (2011).
- [112] J. L. Bohn, M. Cavagnero, and C. Ticknor, *Quasi-universal dipolar scattering in cold and ultracold gases*, New J. Phys. **11**, 055039 (2009).
- [113] B. Gao, *General form of the quantum-defect theory for $-1/r^\alpha$ type of potentials with $\alpha > 2$* , Phys. Rev. A **78**, 012702 (2008).
- [114] P. Langevin, *A fundamental formula of kinetic theory*, Ann. Chim. Phys. **5**, 245 (1905).
- [115] B. Gao, *Universal model for exoergic bimolecular reactions and inelastic processes*, Phys. Rev. Lett. **105**, 263203 (2010).
- [116] A. V. Avdeenkov, M. Kajita, and J. L. Bohn, *Suppression of inelastic collisions of polar $^1\Sigma$ state molecules in an electrostatic field*, Phys. Rev. A **73**, 022707 (2006).
- [117] G. Quéméner and J. L. Bohn, *Shielding $^2\Sigma$ ultracold dipolar molecular collisions with electric fields*, Phys. Rev. A **93**, 012704 (2016).

- [118] M. H. G. de Miranda, A. Chotia, B. Neyenhuis, D. Wang, G. Quéméner, S. Ospelkaus, J. Bohn, J. L. Ye, and D. S. Jin, *Controlling the quantum stereodynamics of ultracold bimolecular reactions*, Nature Physics **7**, 502 (2011).
- [119] A. Frisch, M. Mark, K. Aikawa, S. Baier, R. Grimm, A. Petrov, S. Kotochigova, G. Quéméner, M. Lepers, O. Dulieu, and F. Ferlaino, *Ultracold dipolar molecules composed of strongly magnetic atoms*, Phys. Rev. Lett. **115**, 203201 (2015).
- [120] G. Quéméner, M. Lepers, and O. Dulieu, *Dynamics of ultracold dipolar particles in a confined geometry and tilted fields*, Phys. Rev. A **92**, 042706 (2015).
- [121] A. V. Gorshkov, P. Rabl, G. Pupillo, A. Micheli, P. Zoller, M. D. Lukin, and H. P. Büchler, *Suppression of inelastic collisions between polar molecules with a repulsive shield*, Phys. Rev. Lett. **101**, 073201 (2008).
- [122] S. V. Alyabyshev and R. V. Krems, *Controlling collisional spin relaxation of cold molecules with microwave laser fields*, Phys. Rev. A **80**, 033419 (2009).
- [123] A. V. Avdeenkov, *Dipolar collisions of ultracold polar molecules in a microwave field*, Phys. Rev. A **86**, 022707 (2012).
- [124] C. Ticknor and S. T. Rittenhouse, *Three body recombination of ultracold dipoles to weakly bound dimers*, Phys. Rev. Lett. **105**, 013201 (2010).
- [125] Y. Wang, J. P. D’Incao, and C. H. Greene, *Efimov effect for three interacting bosonic dipoles*, Phys. Rev. Lett. **106**, 233201 (2011).
- [126] Y. Wang, J. P. D’Incao, and C. H. Greene, *Universal three-body physics for fermionic dipoles*, Phys. Rev. Lett. **107**, 233201 (2011).
- [127] M. Lepers, G. Quéméner, E. Luc-Koenig, and O. Dulieu, *Four-body long-range interactions between ultracold weakly-bound diatomic molecules*, J. Phys. B: At. Mol. Opt. Phys. **49**, 014004 (2016).